ADVANCED ENERGY MATERIALS
www.advenergymat.de

Development of Proteins for High-Performance Energy Storage Devices: Opportunities, Challenges, and Strategies

Tianyi Wang, Di He, Hang Yao, Xin Guo, Bing Sun,* and Guoxiu Wang**

In pursuit of reducing environmental impact during battery manufacture, the utilization of nontoxic and renewable materials is essential for building a sustainable future. As one of the most intensively investigated biomaterials, proteins have recently been applied in various high-performance rechargeable batteries. In this review, the opportunities and challenges of using protein-based materials for high-performance energy storage devices are discussed. Recent developments of directly using proteins as active components (e.g., electrolytes, separators, catalysts or binders) in rechargeable batteries are summarized. The advantages and disadvantages of using proteins are compared with the traditional counterparts, and the working mechanisms when using proteins to improve the electrochemical performances of rechargeable batteries are elucidated. Finally, the future development of applying biomaterials to build better batteries is predicted.

1. Introduction

In the past few decades, with rapid growth of energy consumption and fast deterioration of global environment, the social demand for renewable energy technologies is growing rapidly.[1–3] However, the instability and fragility of energy supply from renewable sources (e.g., solar or wind) make the full adoption of renewable energy technologies still a high risk, especially under extreme weather conditions. Developing large-scale energy storage systems (e.g., battery-based energy storage power stations) to solve the intermittency issue of renewable energy sources is essential to achieving a reliable and efficient energy supply chain.[4–8]

T. Wang, D. He, H. Yao
College of Chemistry and Chemical Engineering
Yangzhou University
Yangzhou City, Jiangsu Province 225002, P. R. China
E-mail: yaohang@yzu.edu.cn

X. Guo, B. Sun, G. Wang
Centre for Clean Energy Technology
School of Mathematical and Physical Sciences
Faculty of Science
University of Technology Sydney
Ultimo, NSW 2007, Australia
E-mail: bing.sun@uts.edu.au; guoxiu.wang@uts.edu.au

The ORCID identification number(s) for the author(s) of this article can be found under https://doi.org/10.1002/aenm.202202568.

DOI: 10.1002/aenm.202202568

Currently, traditional lithium-ion (Li-ion) batteries dominate the energy storage market, especially for portable electronic devices and electric vehicles.[9,10] With the increasing demand for building megawatt-scale energy storage systems, the use of Li-ion batteries becomes challenging due to their finite theoretical energy density, safety concerns, and environmental impact during the manufacture process.[11,12] Huge efforts have been devoted to developing new materials and battery chemistries to boost energy densities in the past ten years (**Figure 1**a).[13–20] However, the manufacture of current Li-ion batteries uses a large amount of toxic materials that need to be replaced with more environmentally friendly materials such as biomaterials.[21–23] The direct use of biomaterials as major components for battery manufacturing has attracted significant attention recently (Figure 1b). As classic and important biomaterials, proteins have high biological, chemical, and physical activities, but their structure is simpler than high-dimensional biological tissues (e.g., whole cells). Therefore, proteins have been selected by many research groups as ideal candidates to develop next-generation high-energy rechargeable batteries (Figure 1c).

Herein, in this review, we begin with a brief description of the opportunities and challenges in applying proteins for high-performance rechargeable batteries. Subsequently, we summarize the current research outcomes of using proteins as different battery components, such as electrolytes, separators/interlayers, catalysts, and binders. The advantages and disadvantages of these approaches are elucidated as well. Finally, we predict the future research directions for building better batteries with low environmental impact.

2. Opportunities and Challenges of Proteins in Rechargeable Batteries

For biomaterials in general, three factors are considered as the major limitations for their direct application in rechargeable batteries. i) Biomaterials are very easily denatured by organic solvents and salts in electrolytes.[24,25] ii) The complex composition of biomaterials could cause unpredictable parasitic reactions with other battery components, resulting in irreversible performance deterioration upon cycling.[26] iii) The complex purification processes for biomaterials raises concerns for the pathways to large-scale application in batteries, increasing the predicted costs of commercialization.[27,28] But learning

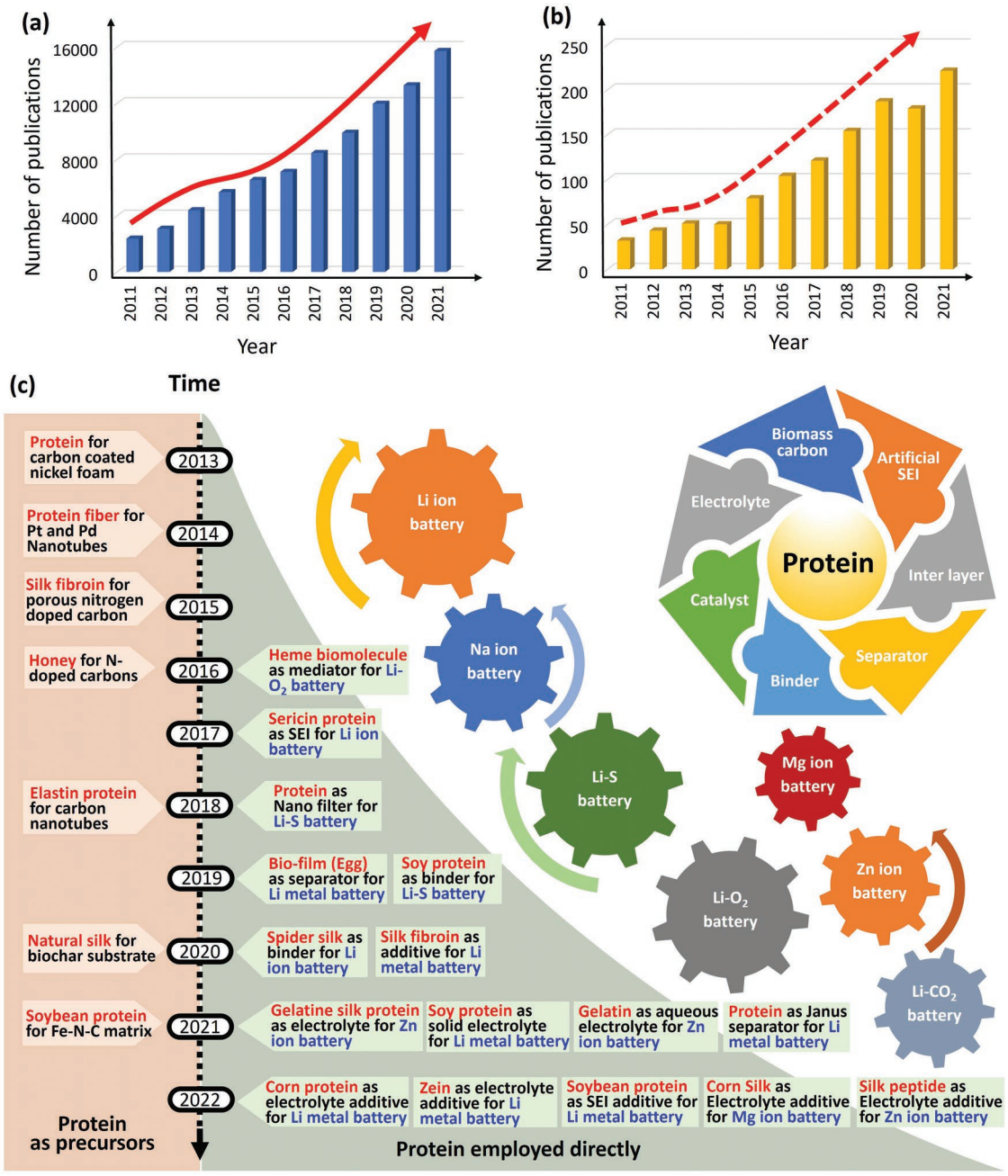

Figure 1. Comparison of the number of scientific publications with the search keyword a) "Battery" and b) "Bio" & "Battery", as searched by Web of Science (July 21, 2022). c) Critical achievements in the development of proteins directly employed (or used as precursors) in new battery designs.

from the development of biochemical industries over several decades, proteins have overcome difficulties in production and purification, and have proven easier to prepare and extract than other higher-dimensional biomaterials.[29,30] This gives a great opportunity to directly utilize proteins in next-generation high-performance rechargeable batteries, such as lithium metal batteries, lithium oxygen/carbon dioxide ($Li–O_2/CO_2$) batteries, and lithium–sulfur (Li–S) batteries.

The functions of the proteins are determined by their complex structures. The amino acid sequence of protein molecules and the 3D structure at different complexity levels permit different functions in rechargeable batteries.[31–33] First, the amino acid sequences of protein–peptide chains are regarded as the primary structure of the proteins (**Figure 2**a). There is an exact amino acid sequence in each type of protein chain, and the peptide bond is the main chemical bond connecting amino acid residues in the primary structure.[33,34] The function of the primary protein structure on battery performance is mainly reflected in the regulation of the internal chemical composition of the battery, such as the formation of SEI layer, participating in the solvation structure of metal ions in the electrolytes, and adsorbing lithium polysulfides in Li–S batteries. Second, the peptide chain in a protein molecule

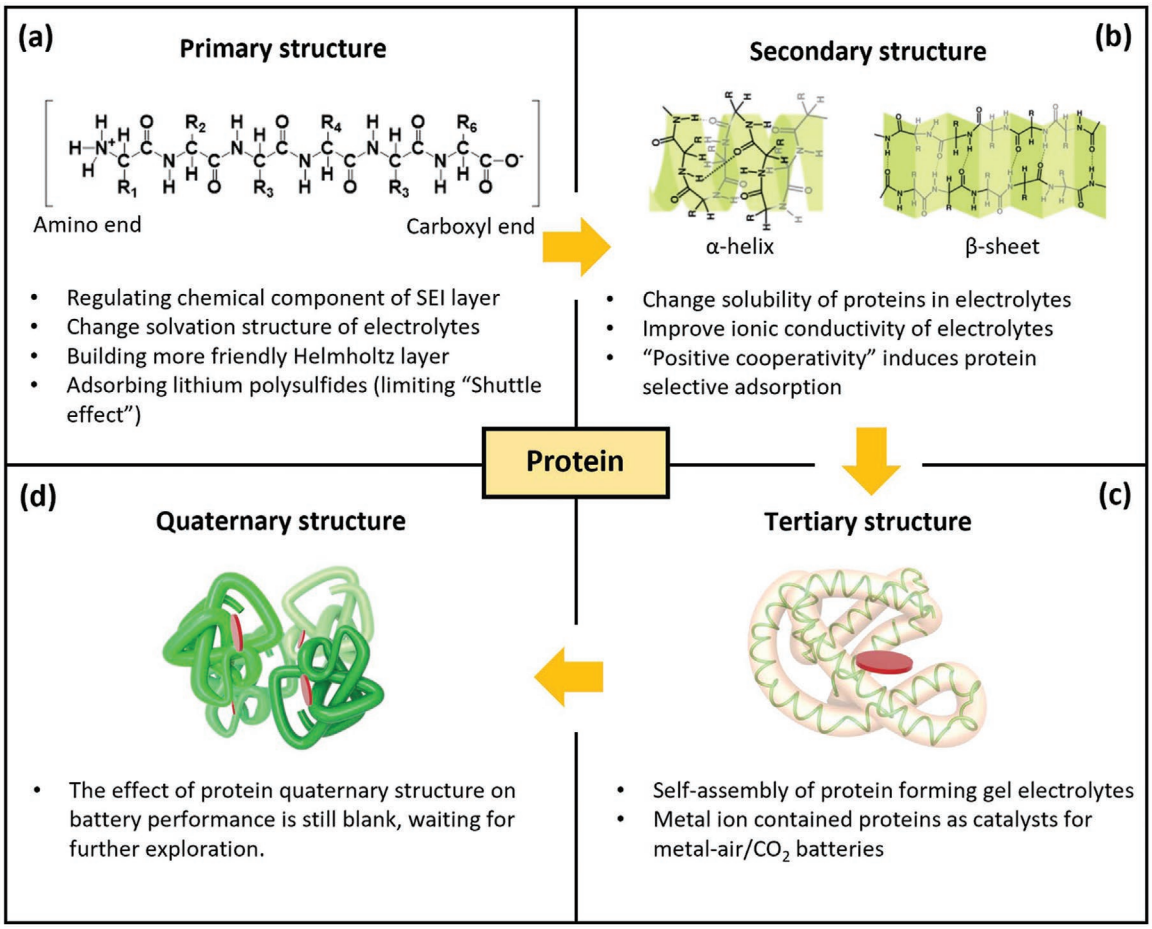

Figure 2. The effect of different levels of protein structure on battery performance and corresponding working mechanisms.

is not a simple straight chain but curled according to specific affinities (e.g., α-helical structure or β-sheet structure), which is identified as the secondary structure (Figure 2b). Hydrogen bonds between the hydrogen atoms on the amino acids' imino (−NH−) groups and the oxygen atoms on the carbonyl groups in the peptide chains construct the protein secondary structure.[35–38] The secondary structure mainly affects the solubility of proteins in the electrolytes, the adsorption–desorption energy of the protein on the surface of electrode materials, and adjusting the distribution of electric field intensity and ionic conductivity of the electrolytes.

In addition, more complex tertiary spatial structures are further constructed by the peptide chains (Figure 2c). The forces that maintain the tertiary structure of globular proteins include van der Waals forces, salt bonds, hydrophobic interactions, and hydrogen bonds, which are collectively referred to as secondary bonds. Furthermore, the disulfide bonds of some proteins also stabilize their spatial structure.[39,40] The contribution of the tertiary structure to the battery performance is reflected as a more dominant factor in the case of gel polymer electrolytes. Finally, a protein spatial structure composed of two or more independent tertiary polypeptide chains may be regarded as the quaternary structures (Figure 2d). Each polypeptide chain unit with a separate tertiary structure is called a subunit. The quaternary structure refers to the 3D arrangement, interaction and contact site layout of subunits.[41,42] However, to date, the effect of protein quaternary structure on battery performance is still undocumented, awaiting further exploration.

Although proteins have been successfully used in several advanced rechargeable battery systems, the following challenges still constrain their future development.

i) The vulnerability of proteins. Compared with their native biological environment, the chemical environment in some batteries, especially in nonaqueous electrolytes, is unfriendly to proteins. Organic solvents, highly concentrated salts, and strong electric fields easily cause inactivation and even decomposition of proteins.
ii) Influence of impurities. Due to the vulnerability of the internal electrochemical reactions of rechargeable batteries, contaminants such as water and oxygen can cause severe parasitic reactions during charge/discharge processes, especially at high temperatures. Proteins often contain crystal water, and their purification process is complex. The addition of proteins in rechargeable batteries could induce parasitic reactions that may deteriorate the electrochemical performance of rechargeable batteries.
iii) Unclear working mechanisms. The structure of proteins is complex and fragile, which poses a significant challenge for studying their working mechanisms. Fortunately, in recent

years, with the development of advanced characterization techniques, the direct application of proteins in batteries has been boosted. For example, a cryo-electron microscope (Cryo-EM) can be used to characterize chemically reactive and sensitive samples at an extremely low temperature (–185 °C) and low dose exposure, thus reducing the damage from electron beam irradiation. The confocal laser scanning microscope (CLSM) can perform high-precision 3D characterization on proteins in a nondestructive state. Assisted by CLSM, the details of protein attachment on the electrode surface can be more clearly observed under UV irradiation.

3. Proteins as Major Components of Electrolytes

Electrolytes in rechargeable batteries play an essential role in supporting the transport of metal ions between the two electrodes. An ideal electrolyte is an excellent conductor of metal ions but an insulator of electrons.[43–45] Currently, the commonly used electrolytes can be divided into organic electrolytes and aqueous electrolytes. They can also be divided into liquid, quasi-solid, and solid-state electrolytes according to their physical states. Optimizing the composition of electrolytes with natural abundant and nontoxic materials to replace the toxic materials in traditional electrolytes has become one of the hot topics in this research area.[46] Therefore, using nontoxic proteins as major components to directly prepare electrolytes for rechargeable batteries has been intensively reported in different battery systems recently (**Table 1**).[47–54] Moreover, as a representative of biological macromolecules, the unique self-assembly properties of proteins at the molecular level show immense potential for designing aqueous electrolytes.

The application of proteins to prepare electrolytes can be traced back to 2018. Li et al. first filled polyacrylamide (PAM)-grafted gelatin hydrogel onto a polyacrylonitrile fiber membrane to obtain a hierarchical polymer electrolyte (HPE) (**Figure 3**a).[47] Gelatin is also the most widely used protein for electrolyte applications. As shown in Figure 3b, the obtained HPE is a uniform film with excellent flexibility. The thickness of the resulting electrolyte membrane is ≈30 µm with a 3D porous morphology derived from the gelatin-g-PAM hydrogel. The flexibility of the electrolyte film facilitates the fabrication of flexible batteries, while its 3D porous structure provides abundant pathways for ion transport during cycling. When applied in Zinc-ion (Zn-ion) batteries, the cell using HPE exhibited a high initial discharge capacity of 275 mAh g^{-1} at 61.6 mA g^{-1}, high Coulombic efficiencies at different current densities, and a discharge capacity of 269 mAh g^{-1} at 1 C after 40 cycles (Figure 3c). At a super high current density of 2772 mA g^{-1}, the cell maintained a high retention of 97% after 1000 cycles. The excellent electrochemical performance of the cells with HPE is based on the following three factors. 1) The excellent wettability of the as-prepared HPE toward electrodes. 2) The 3D highly porous structure and strong liquid holding capability of HPE. 3) Synergistic effects derived from the well-dispersed CNTs and MnO_2 composite electrodes. In the same year, Han et al. synthesized gelatin hydrogel electrolyte (GHE) using a facile fast-cooling method.[48] GHEs with certain shapes can be obtained by pouring a 60 °C gelatin solution into a mold for cooling. When the temperature is higher than the gelation temperature (T_g), gelatin molecules can be regarded as random coils. However, these molecules are locally aggregated to construct helical segments during the cooling process. The gelatin protein molecules with α-helix second structures can coil and form fibers, which finally construct a solid-state network.[56,57] A fast-cooling process is essential to enhance the mechanical strength against external destructive forces (e.g., cutting, bending, twisting, and crimping) because less ordered gelatin molecules can be obtained at a high cooling rate, implying less crystallinity (and hence, less brittleness) and more fluid-like structure. As shown in Figure 3d, due to the high plasticity of gelatin, solid-state Zn metal batteries with both sandwiched and interdigitated configurations can be constructed using GHE-coated $LiMn_2O_4$ as the cathode and Zn foil as the anode. The GHE can support an excellent ionic conductivity of 6.15 mS cm^{-1} (Figure 3e). In addition, the Zn anode in GHE shows much lower corrosion behavior (10.23 µA cm^{-2}) than the Zn anode in normal aqueous electrolyte (43.06 µA cm^{-2}) (Figure 3f), indicating that GHE

Table 1. Protein-based electrolytes and electrolyte additives in rechargeable batteries.

Electrolytes	Applications	Ionic conductivity [S m^{-1}]	Cathodes	Anodes	Electrochemical performances	Refs.
Gelatin/PAM-based solid-state electrolyte	Zn-ion battery	1.76	α-MnO_2/CNT	Zn/CNT	97% capacity retention at 2772 mA g^{-1} after 1000 cycles	Ref. [47]
Gelatin-based hydrogel electrolyte	Zn metal battery	0.61	$LiMn_2O_4$	Zn metal	≈100 mAh g^{-1} at 25 mA g^{-1} after 100 cycles	Ref. [48]
Gelatin-based solid-state electrolyte	Zn-ion battery	1.6 to 0.4	MnO_2	Zn metal	90% capacity retention at 1540 mA g^{-1} after 500 cycles	Ref. [50]
Zein-based gel electrolyte	Li–S battery	0.21	Sulfur	Li metal	635 mAh g^{-1} at 1000 mA g^{-1} after 400 cycles	Ref. [51]
Soybean protein-based solid polymer electrolyte	Li-ion battery	0.0256	$LiFePO_4$	Li metal	55 mAh g^{-1} at ≈85 mA g^{-1} after 100 cycles	Ref. [52]
Sulfonated bacterial cellulose-based gel electrolyte	Li–O_2 battery	0.016	O_2	Li metal	500 mAh g^{-1} at 200 mA g^{-1} after 60 cycles	Ref. [53]
Corn silk-based solid-state electrolyte	Mg-ion battery	0.0128	MnO_2	Mg metal	1.2 mAh in primary battery	Ref. [54]
Gelatin-based electrolyte	Zn-ion battery	3.7	MnO_2	Zn metal	212 mAh g^{-1} at 2000 mA g^{-1} after 200 cycles	Ref. [55]

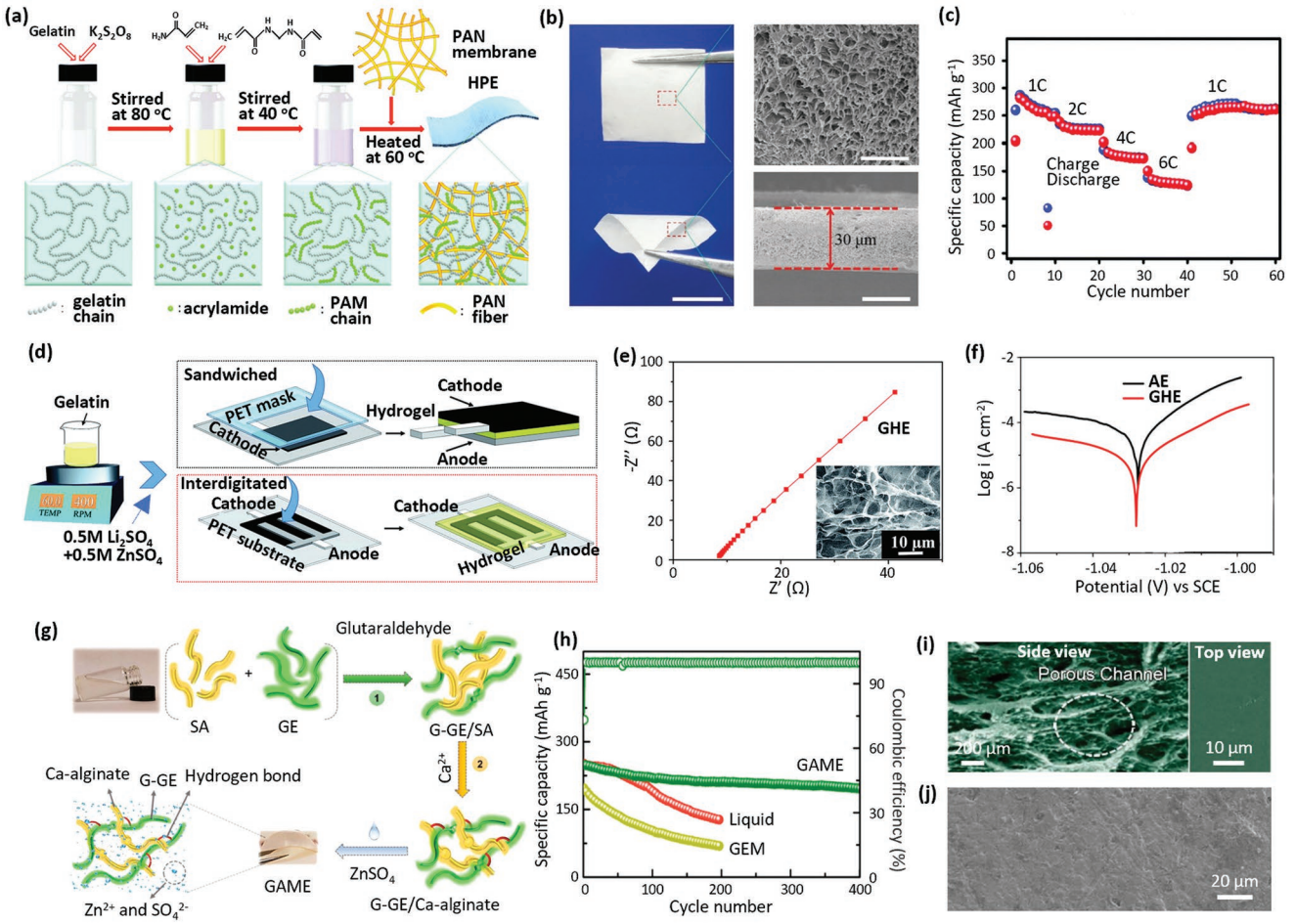

Figure 3. a) Schematic illustration of the preparation of hierarchical polymer electrolytes. b) Optical and SEM images of PAM-grafted gelatin electrolyte films. c) Rate performance of Zn-ion batteries with PAM grafted gelatin electrolyte films. Reproduced with permission.[47] Copyright 2018, Royal Society of Chemistry. d) Schematic illustration of assembled cells with sandwiched and interdigitated configurations. e) EIS plots and SEM images of gelatin hydrogel electrolyte (GHE). f) Comparison of Tafel plots of the Zn electrodes in the aqueous electrolyte and GHE. Reproduced with permission.[48] Copyright 2018, Royal Society of Chemistry. g) Schematic of the overall preparation process of GAME. h) SEM images of frozen-dried GAME from different viewpoints. h) Cycling performance of the cells with GAME, GEM and liquid electrolytes at 2 A g^{-1}. j) Surface of Zn foil after 150 cycles at 1 A g^{-1} with GAME. Reproduced with permission.[55] Copyright 2019, American Chemical Society.

can facilitate the smooth deposition of Zn metal. Thus, the Zn‖GHE‖Zn symmetrical cells maintained stable cycling stability for more than 800 h at 0.2 mA cm^{-2}.

In 2019, Lu et al. synthesized a 3D gelatin-sodium alginate membrane electrolyte (GAME).[55] As shown in Figure 3g, the advantages of gelatin/sodium alginate GE/SA, including high modulus of SA and the hydrophilicity of GE with high dielectric strength, have been utilized to develop a flexible and robust Zn^{2+}-ion conductive semisolid polymer electrolyte layer through two crosslinking reactions. A large number of polar carboxyl and hydroxyl groups of the GE/SA composite facilitated the formation of an interpenetrated 3D network with inorganic salt dissociation after being immersed in $ZnSO_4$ solution. When applied in Zn-ion batteries with V_2O_5 as the cathode material, a high capacity of 212 mAh g^{-1} can be maintained after 200 cycles, corresponding to 85% of its initial discharge capacity (Figure 3h). The cross-sectional SEM images of the GAME after freeze-drying show the interconnected porous channels within the network (Figure 3i). The porous 3D structure is beneficial for accommodating $ZnSO_4$ solution. As shown in Figure 3j, the surface of the cycled Zn foil with GAME is still very smooth without Zn dendrites after cycling. The authors explained the improved electrochemical performance could be contributed by the high ionic conductivity and high mechanical resistance to Zn dendrite growth due to the participation of GAME.

The self-assembly characteristics of proteins can also assist in synthesizing electrolytes with specific properties. In 2019, Han et al. reported a gelatin-based solid-state electrolyte (GSE) for solid-state Zn-ion batteries using a unique quick-cooling technique to change the conformation of the gelatin chain from disordered to ordered (**Figure 4**a).[50] Notably, the GSE exhibited superior mechanical strength after being immersed in $ZnSO_4$ solution. Stress–strain experiments demonstrated the interaction effect between the tensile strength of the GSE samples and the concentrations of $ZnSO_4$ solution (Figure 4b). At a strain of 560%, the GSE treated with 2.5 M $ZnSO_4$ solution (denoted as GSE-2.5) had a fracture tensile strength of 2.78 MPa. When applied in Zn‖Zn symmetric cells, the GSE-2.5 demonstrated

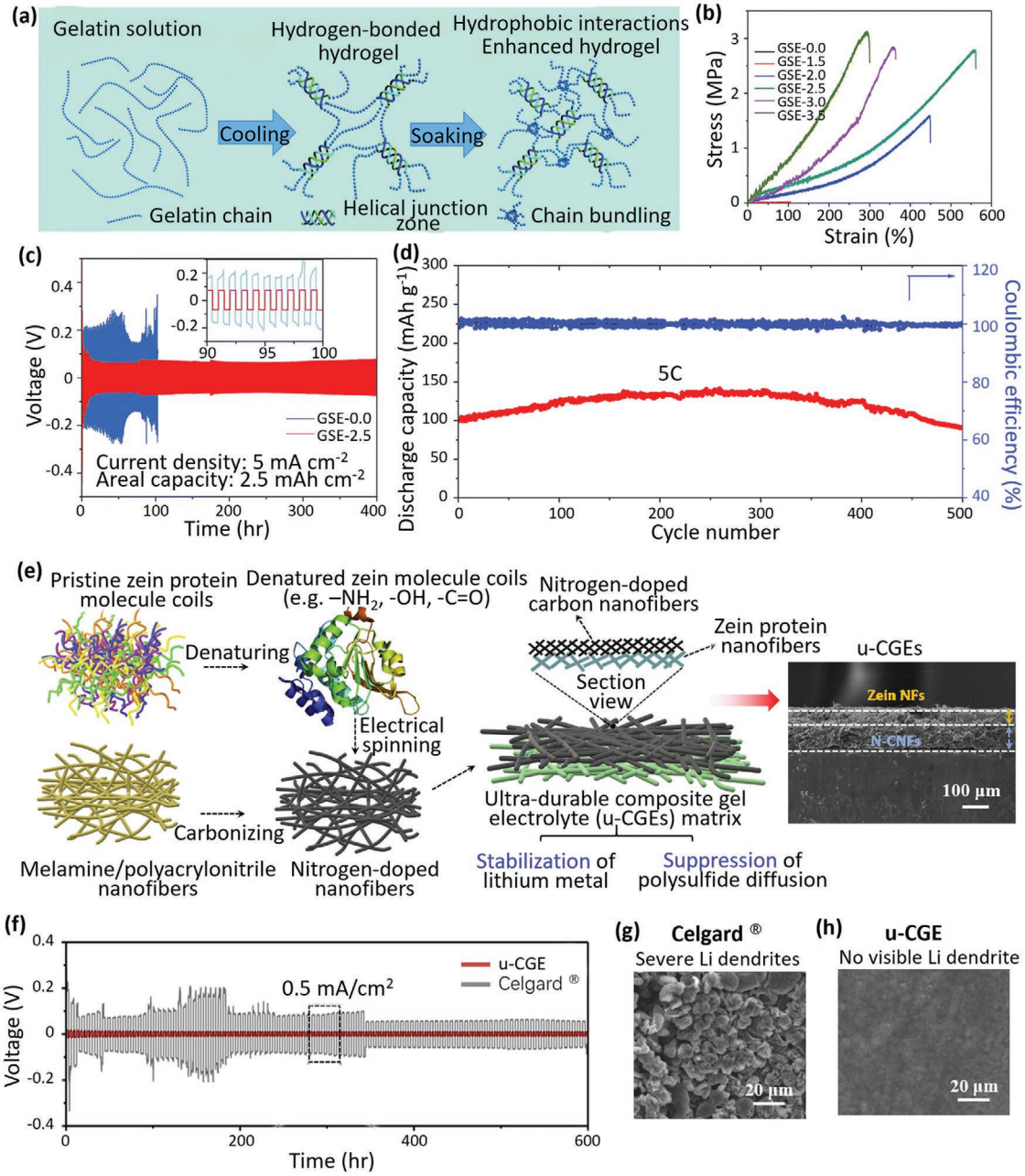

Figure 4. a) Schematic illustration for preparing salt-reinforced GSE. b) Stress–strain curves of GSE treated with different concentrations of $ZnSO_4$ solution (0–3.5 M). c) Galvanostatic discharge–charge voltage curves of Zn||GSE-0.0||Zn and Zn||GSE-2.5||Zn sympatric cells at 5 mA cm^{-2} with capacity limitations of 2.5 mAh cm^{-2}. d) Cycling performance of Zn||GSE-2.5||MnO_2 full cell at 5 C. Reproduced with permission.[50] Copyright 2019, Royal Society of Chemistry. e) Illustration of the preparation process of u-CGE and SEM image of a cross-sectional view of u-CGE. f) Galvanostatic cycling test of Li||u-CGE||Li and Li||Celgard||Li symmetric cells at 0.5 mA cm^{-2}. g,h) SEM image of retrieved Li anodes from Li||Celgard||Li and Li||u-CGE||Li cells. Reproduced with permission.[51] Copyright 2018, Elsevier.

a fluent voltage charge–discharge profile and good cycling stability at 5 mA cm^{-2} for more than 400 cycles (Figure 4c). Owing to the restricted concentration of free water in GSE-2.5, the side reactions such as hydrogen evolution reaction (HER) were significantly suppressed. Figure 4d shows that the excellent mechanical strength of GSE-2.5 significantly improved the cycling stability of Zn-ion batteries by 90% for 500 cycles at a rate of 5 C.

In addition to enhancing the stability of the electrolytes, the abundant heteroatom-containing functional groups on proteins can adsorb intermediate species in batteries, thus further improving the service life of the batteries. In 2020, Ding et al. designed an ultradurable composite gel electrolyte (u-CGE) for Li–S batteries to inhibit polysulfide diffusion from the sulfur cathode side to the Li metal anode side.[51] Figure 4e shows how the u-CGE was prepared by electrospinning denatured

zein protein molecules onto nitrogen-doped carbon nanofibers (N-doped CNFs). The zein nanofibers with an average diameter of 250 nm showed a rough interconnected 3D nanofibrous morphology. The ultrafine nanofibrous system promised a hierarchical porous structure and an improved specific surface area of CGEs, and the N-doped CNFs and zein protein showed good compatibility. When applied in Li‖u-CGE‖Li symmetric cell, the battery maintained a low overpotential of 3 mV at 0.5 mA cm^{-2} and a stable cycling performance for more than 600 h (Figure 4f). By contrast, a Li‖Celgard‖Li symmetric cell without u-CGE showed high and unstable overpotentials that exceeded 100 mV. This is because the u-CGE can greatly enhance the stability of the surface environment of Li metal anode (Figure 4g,h). The N-containing peptide groups of the zein protein molecules absorb Li^+ ions by polar groups and capture molecules of the electrolyte solvent, resulting in more restriction of anions and promoted transportation of Li^+ ions.

The abundant hydrophilic/hydrophobic functional groups of proteins allow their use in quasi-solid-state electrolytes but limit their further application in solid-state electrolytes. Mixing proteins with lithium salt has been proven effective in overcoming this obstacle. In 2020, Zhou et al. synthesized a new polyvinylidene fluoride (PVDF)–soybean protein isolate (SPI)–montmorillonite (MMT) solid electrolyte.[52] An appropriate amount of LiTFSI was evenly added into *N,N*-dimethylacetamide (DMAc) solution containing PVDF, SPI, and MMT. Then, the mixed solution was cast on a glass plate and cut into small pieces after evaporation of the solvent. From the SEM images (**Figure 5**a), a uniform spherical structure can be seen in the electrolyte membrane after the addition of SPI and MMT, indicating that the electrolyte membrane materials were well compatible. The tensile strength testing results also demonstrated that the addition of SPI significantly enhanced the mechanical property of the polymer electrolytes (Figure 5b). Electrochemical testing results showed that the Li‖PVDF–SPI–MMT–LiTFSI‖Li cell maintained stable cycling performance for more than 100 h at 0.05 mA cm^{-2}. The overpotential is only about 200 mV, which is much smaller than that of the Li‖PVDF–LiTFSI‖Li cell (>400 mV) (Figure 5c). In addition, the $LiFePO_4$‖Li full cell with PVDF–SPI–MMT–LiTFSI electrolytes also exhibited much-improved cycling performance (Figure 5d).

Shi et al. made sulfurized bacterial cellulose (SBC) into a gel electrolyte for Li–O_2 batteries.[53] The SBC has abundant $-SO_3^-$ groups, which can generate electrostatic repulsion toward I_3^- ions in the electrolyte, thereby inhibiting the "shuttle effect" of Li–O_2 cell (Figure 5e). Compared with pristine bacterial cellulose (BC), a denser fibrous and porous structure keeps the surface of SBC smooth and flat after soaking in dimethyl sulfoxide (DMSO) solvent for three days. In the energy dispersive spectroscopy (EDS) mapping of SBC, the distributions of C, O, and S elements are homogenous, indicating a successful sulfonation of the SBC (Figure 5f). In Li–O_2 battery application (Figure 5g), batteries using SBC gel polymer electrolyte showed the longest cycling life (60 cycles), surpassing that of Li–O_2 batteries with BC gel polymer electrolyte and conventional liquid electrolyte.

Apart from monovalent-ion batteries, the solid-state electrolytes prepared from proteins can also be used in multivalent-ion batteries.[58] Suvarna et al. prepared a biopolymer electrolyte film using corn silk extract (CSE), a common biological waste.[54] Due to the weak film-forming ability of CSE, the author added $MgCl_2$ into highly dispersed polyvinyl alcohol (PVA) and CSE solution in petri dishes to obtain solid biopolymer films. From Nyquist plots, an appropriate ratio of CSE and PVA can reduce impedance and alleviate the polarization of Mg electrodes. The electrochemical characterization results indicate that 1 g PVA and 0.9 g CSE is the best mixing ratio with the highest ionic conductivity (1.74×10^{-5} S cm^{-1}). A primary Mg-ion battery was successfully assembled with the optimized PVA/CSE solid-state electrolytes.

In summary, the working mechanism of proteins in different electrolytes is completely different. In the organic electrolyte system, proteins exist in the form of micelles because it is difficult for proteins to assemble as the gel in the organic environment. However, in the aqueous electrolyte system, proteins can easily form a quasi-solid-state gel via self-assembly and hydration. These protein gels with very ordered grid structures can facilitate the ion transport during change and discharge processes. Furthermore, in aqueous electrolyte, some proteins can chelate with multivalent ions through complexation to realize a higher homogeneous deposition. Compared with other conventional electrolytes, employing proteins as the major components to prepare electrolytes shows many advantages. First, most proteins are nontoxic and harmless. Unlike industrial organic solvents, the electrolytes using protein are safer and more environmentally friendly. Second, a large number of nitrogen-containing functional groups in the protein can effectively guide the transmission of metal ions and reduce the internal polarization of the battery. Third, some proteins can form quasi-solid electrolytes with good mechanical properties after self-assembly or mixing with other polymers. These can prevent electrolytes from leakage and inhibit any dendrite formation on the surface of metal anodes, which could significantly improve the service life of rechargeable batteries. However, a disadvantage of using some proteins may be the cost to produce. Moreover, some proteins may chelate with divalent metal ions and thus interfere with the kinetics of ion transport in the battery.

4. Proteins as Electrolyte Additives

The development of electrolyte additives that can improve electrochemical performances over the existing electrolyte systems has become increasingly attractive recently.[59–64] The advantages of using additives are low preparation cost, easy processing, and minimum influence on the battery's interior environment. For example, in 2021, Han et al. investigated the influence of adding gelatin into an aqueous electrolyte in Zn-ion batteries.[61] The authors discovered that an optimized amount of gelatin added to electrolytes could effectively improve the charge/discharge Coulombic efficiencies of batteries, thus extending the cycling stability of the batteries. When the addition of gelatin was increased from 0 to 3.5 g L^{-1}, a high Coulombic efficiency of Zn-ion batteries can be maintained to above 1000 cycles.

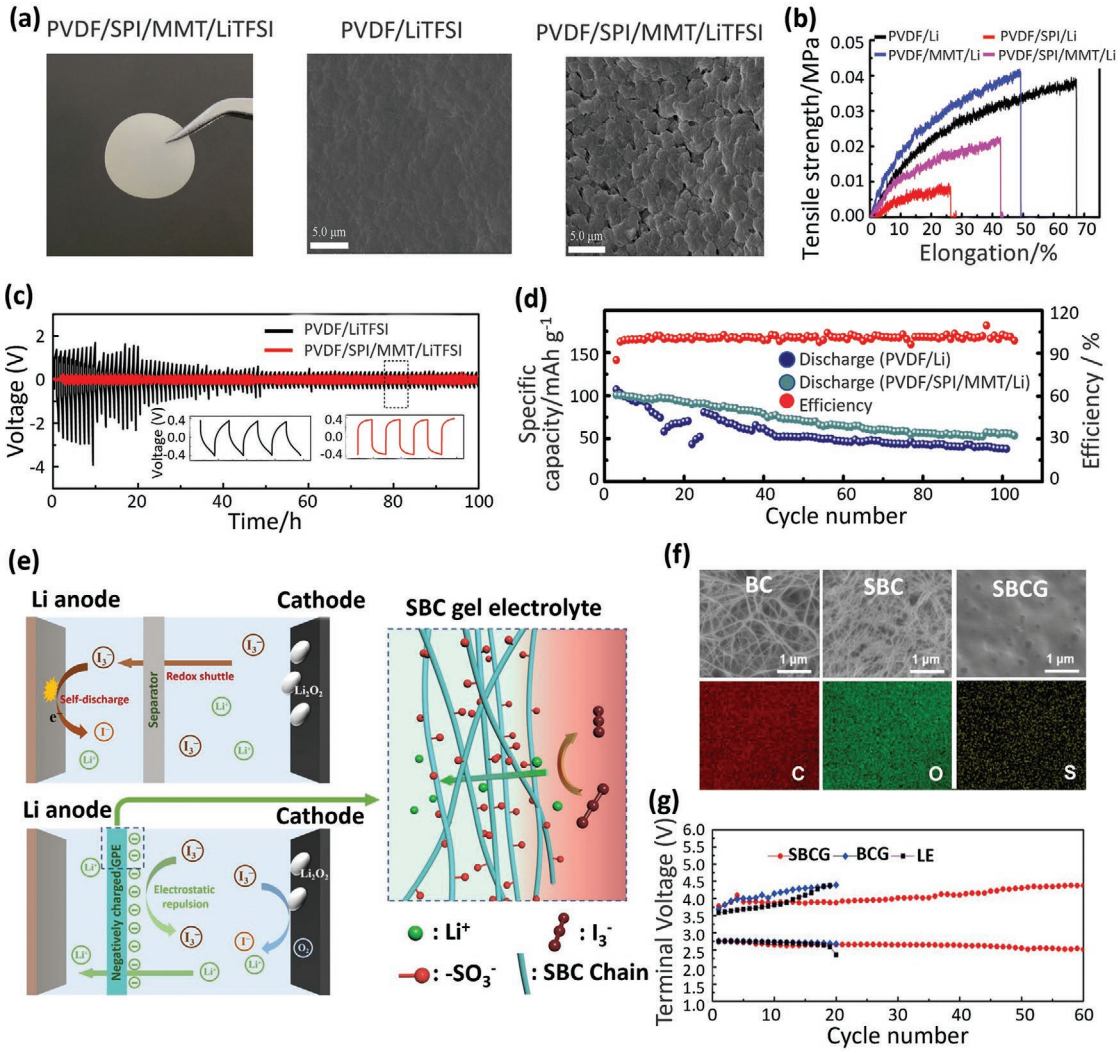

Figure 5. a) Optical photo of PVDF/SPI/MMT/LiTFSI solid polymer film, SEM images of PVDF–LiTFSI and PvDF/SPI/MMT/LiTFSI solid polymer films. b) Mechanical properties of different electrolytes, tensile strength versus elongation. c) Galvanostatic cycling tests of Li‖PVDF/LiTFSI‖Li and Li‖PVDF/SPI/MMT/LiTFSI‖Li cells at 0.05 mA cm^{-2}. d) Cycling performance of cells with different electrolytes. Reproduced with permission.[52] Copyright 2020, Springer Nature. e) Schematic illustration for SBC inhibiting the "shuttle effect" of LiI RM. f) SEM of BC, SBC, and SBCG (after soaking in DMSO liquid for three days). EDS mapping of SBC. g) Cycling performances of Li–O_2 cells with different electrolytes (terminal voltages vs cycle number). Reproduced with permission.[53] Copyright 2011, American Chemical Society.

However, when the concentration of gelatin in the electrolyte reached 7.0 g L^{-1}, a serious decline in Coulombic efficiency occurred. The authors explained that gelatin could improve the electrochemical performance of Zn metal anodes because the gelatin molecules adhere to the surface of the Zn anodes and homogenize the Zn^{2+} ion deposition, thus suppressing Zn dendrite formation. However, when the concentration of the gelatin additive is too high, the free Zn^{2+} ions will combine with the acetate ions in the solution, reducing the Zn^{2+} ion concentration that can participate in charge/discharge cycles. A similar protective mechanism was also employed in Li-ion batteries. In 2022, Wang et al. directly used zein as an electrolyte additive for Li metal batteries to alleviate lithium dendrite growth.[65] They found that the dissolved zein can be immobilized on the surface of the Li anode, which repairs the broken SEI and inhibits Li dendrite growth (**Figure 6**a). The repaired SEI possessed better mechanical and electrochemical properties because the nitrogen-containing functional groups of zein can attract PF_6^- to construct a better Helmholtz layer to absorb Li^+ ions. The modified SEI layer can alleviate the inhomogeneous deposition of Li ions and prolong the cycle life of Li metal anodes. SEM images of Li metal anodes before and after 25 cycles (Figure 6b) show the surface of the Li foil cycled in zein-containing electrolyte has a smoother morphology than its non-zein counterpart. In Li‖Li symmetric cell testing, the cell with zein additive achieved a much longer cycle life of about 420 h than the cell without additive (≈280 h) at the same current density, and this was true across a wide range of current densities (Figure 6c). When applied in Li‖$LiFePO_4$ full cells, the cell with zein additive achieved a discharge capacity of 83.8 mAh g^{-1} at 2 C after

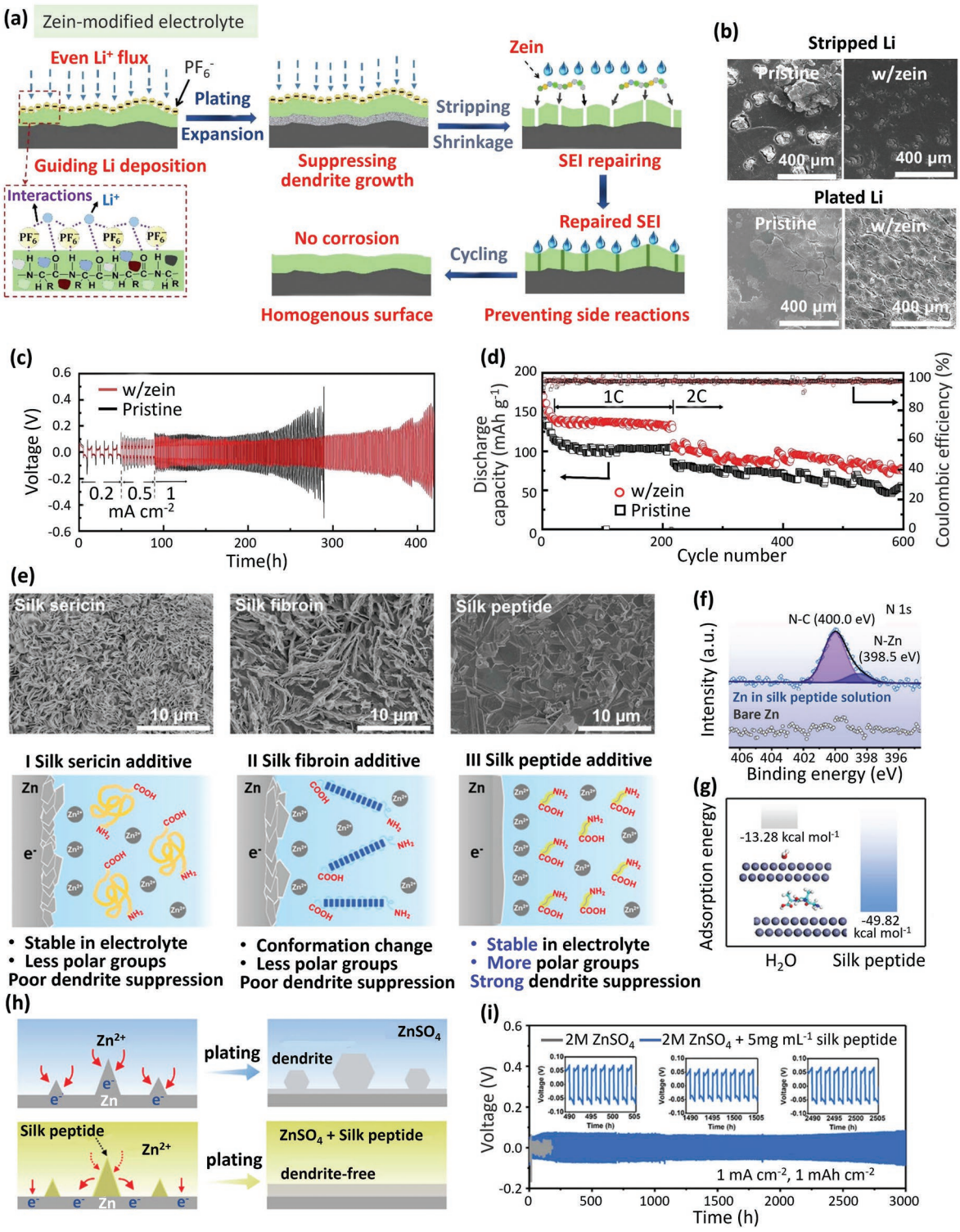

Figure 6. a) Schematic illustration of zein additive reducing the growth of Li dendrites. b) SEM images of pristine and cycled Li anodes with and without zein additive. c) The cycling performances of symmetric Li||Li symmetrical cells with and without zein additive at different current densities. d) Long cycling performance of Li||$LiFePO_4$ full cell with and without zein additive. Reproduced with permission.[65] Copyright 2022, Elsevier. e) Zn deposition morphology characterization and the corresponding reaction mechanisms suppressing Zn dendrites with three different additives. f) XPS spectra of N 1s peak of Zn foil after soaking in silk peptide solution. g) Density functional theory calculation results of the adsorption energy of H_2O and silk peptide on Zn (002) surfaces. h) Schematic illustration of the electrostatic shielding effect of silk peptide for suppressing Zn dendrite growth. i) The cycling performances of Zn||Zn symmetric cells using $ZnSO_4$ electrolytes with or without silk peptide additive (5 mg mL^{-1}). Reproduced with permission.[62] Copyright 2022, Wiley-VCH.

600 cycles, corresponding to 46.6% of the initial capacity, while the reversible capacity ratio of the counterpart using pristine electrolyte was just 36.4% (Figure 6d).

Due to the large molecular weight and complex structure of proteins, the solubility of proteins has always plagued their dispersion as electrolyte additives. Reducing the molecular weight of proteins but still maintaining their chemical properties has become a new strategy. In 2022, Wang et al. used silk peptide as an electrolyte additive in 2 M $ZnSO_4$ electrolyte to suppress the growth of Zn dendrites.[62] The silk peptide was obtained by hydrolysis of silk fibroin, which keeps the abundant $-NH_2$ and $-COOH$ groups and improves the fibroin solubility in aqueous electrolytes. The Zn deposition morphologies showed Zn dendrites still grew when plain sericin and plain (i.e., long-chain) fibroin were added to $ZnSO_4$ electrolytes (Figure 6e). By contrast, when short-chain fibroin was used, Zn was deposited smoothly and parallel to Cu substrates without obvious dendrite formation. The authors explained that the short-chained silk peptide molecules showed more exposed carboxylic and amino groups and better solubility in aqueous $ZnSO_4$ electrolytes compared with long-chained silk sericin and fibroin molecules. This could facilitate the desolvation of Zn ions, which resulted in homogenous Zn nucleation and growth. The XPS spectra and density functional theory calculation results indicated the strong interaction between the Zn metal and the polar groups of silk peptide (Figure 6f,g). In addition, the authors also suggested that silk peptide could produce an electrostatic shielding effect on Zn metal dendrite, reducing the diffusion speed of Zn^{2+} ions near the tips of the dendrites and promoting the uniform deposition of Zn^{2+} ions on Zn metal (Figure 6h). Zn||Zn symmetrical cells with silk peptide additive shows a stable cycle life of more than 3000 h at a current density of 1 mA cm^{-2} with the capacity limitation of 1 mAh cm^{-2}. By contrast, cells without silk peptide additive were short-circuited by about 120 h (Figure 6i). This work confirms that using small molecules such as silk peptide with abundant polar functional groups to enhance the performance of aqueous Zn-ion batteries is a facile and effective strategy.

In addition, using synergistic effect from different additives to suppress both corrosion and dendrite formation of Zn anodes was also investigated. For instance, Liu et al. investigated the protection capability of gelatin on electrodes in aqueous Zn-ion batteries.[66] As shown in **Figure 7**a, the addition of $MnSO_4$ and gelatin significantly changed the deposition behavior of Zn metal. When Zn was deposited in pristine electrolyte (2 M $MnSO_4$), the deposited Zn preferred to grow along (112) planes. After the addition of Mn^{2+} ions in the electrolytes, the crystal orientations of the deposited Zn change to (103) and (002) planes. Furthermore, with the addition of both $MnSO_4$ and gelatin in the electrolyte, the decreased XRD reflected intensities of almost all crystalline planes were observed on deposited Zn metal, confirming that numerous gelatin molecules were adsorbed on the surface of Zn metal anode and significantly changed the deposition behaviors of Zn^{2+} ions. As shown in Figure 7b, when applied in a Zn||Zn symmetric battery at 0.25 mA cm^{-2}, the electrolyte containing both gelatin and Mn^{2+} ions demonstrated significantly extended cycling stability. In full cell applications, after 1000 cycles at 500 mA g^{-1}, the capacity retention of Zn||MnO_2 with gelatin and Mn^{2+} coadditive was 79.6%. By contrast, the capacity retention of Zn||MnO_2 cell without any additive was only 6.3% (Figure 7c).

The protective effect of protein additive in organic electrolytes on alkali metal anodes has also been systematically investigated. Wang et al. chose fibroin as the additive for ether-based electrolytes and analyzed the interaction between fibroin molecules and Li metal anodes (Figure 7d).[67] According to their investigations, fibroin molecules exist as micelles of α-helix secondary structures in ether-based electrolytes. Under the driving force of an electric field, the charged protein molecules migrate to the Li anode side autonomously and transform from α-helix into β-sheet secondary structures once contacting the surface of a Li metal anode (Figure 7f). After the secondary structure changes, the hydrophobic functional groups inside the protein will be "expanded," which will enhance the adsorption effect of the protein molecules on the Li metal surface, especially in regions with large curvatures such as edges and tips (Figure 7g). SEM images of deposited Li on Cu foils show dense and uniform morphology, indicating the addition of protein can reduce parasitic reactions and suppress dendrite formation (Figure 7e). Cryo-EM images demonstrate that the fibroin layer can be clearly detected on the surface of SEI layers on Li metal anodes. Moreover, proteins adsorbed on the surface of lithium metal will participate in forming an SEI film on the surface of lithium metal. Compared with the SEI layer formed in the pristine electrolyte without additives, the SEI layer formed in fibroin-containing electrolytes shows increased amounts of α-Li_3N. This can enhance the mechanical properties of the SEI layer and support a more stable electrolyte/electrode interface, resulting in much-improved cycling stability in both Li||Li symmetric cells and Li||Cu half cells (Figure 7h,i). Finally, the authors prepared (by electrospinning) a membrane that could release fibroin slowly, which overcame the disadvantage of the low solubility of fibroin in their ether-based electrolyte.

In conclusion, when used as electrolyte additives, proteins participate in the formation of protective layers on both cathodes and anodes. The small amount of protein additive could move freely in liquid electrolytes to achieve a dynamic protection effect and reduces the production cost as well. In the traditional research on proteins, buffer solution often plays an essential role in enhancing the stability of protein molecules in the aqueous environment. The appropriate use of buffer solution can protect the integrity of the proteins while separating them from other integrated cell components. However, due to the complicated chemical environment inside batteries, the study of protein additives with buffer solution has not been reported yet. The traditional buffer solution theory is based on aqueous solutions, which might not be suitable for nonaqueous electrolytes. Fortunately, with the rapid development of next-generation aqueous electrolytes, we predict that the combination of proteins and buffer solution as additives in aqueous electrolytes could become a possible strategy

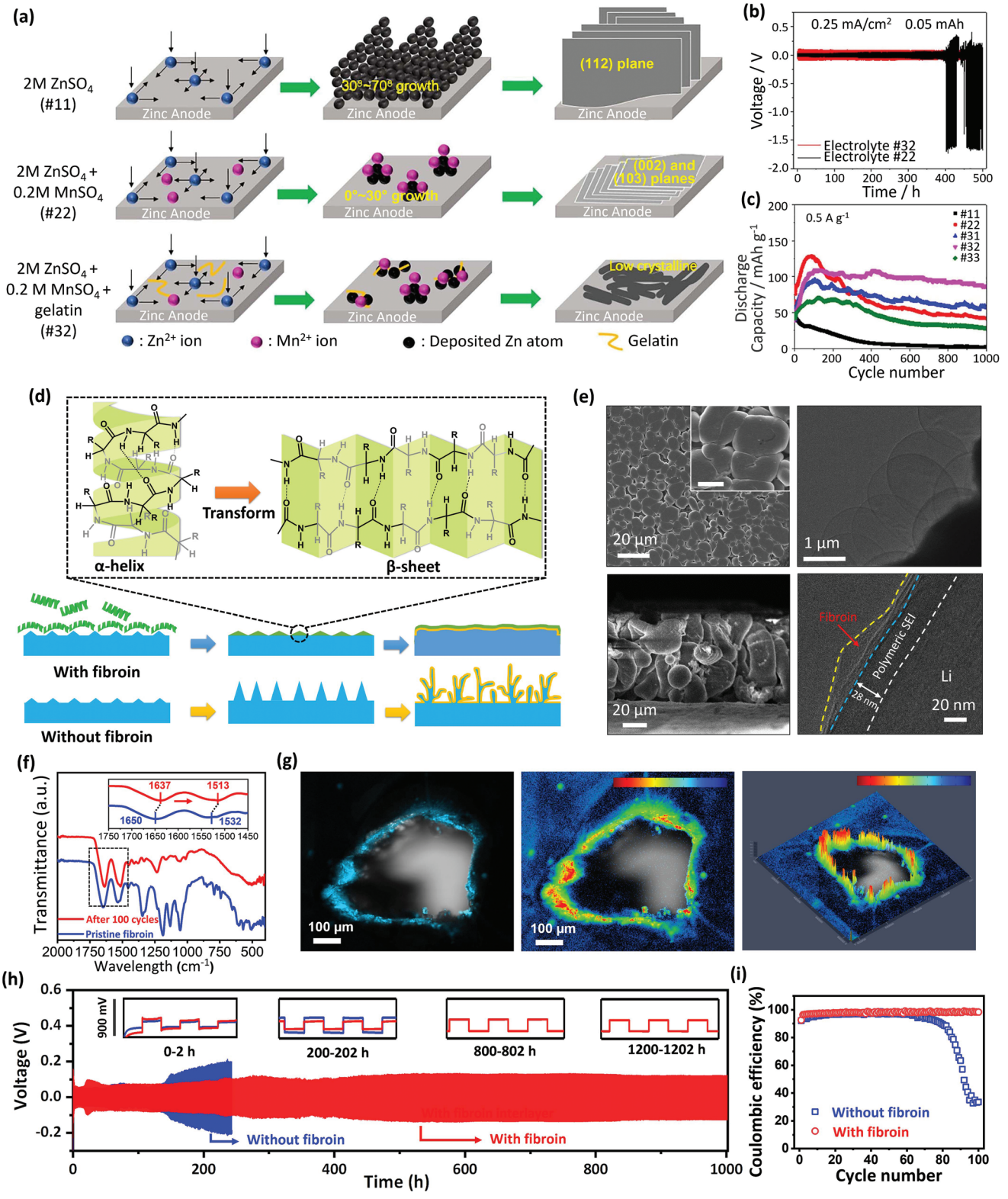

Figure 7. a) Working mechanism of gelatin/Mn^{2+} coadditive for suppressing the growth of Zn dendrites. b) Long-term cycling performance of Zn‖Zn symmetric cells with different electrolytes. (#22:2 M $ZnSO_4$ + 0.2 M $MnSO_4$; #32:2 M $ZnSO_4$ + 0.2 M $MnSO_4$ + 0.5% gelatin). c) Cycling performance of Zn‖MnO_2 full cells with various electrolytes. Reproduced with permission.[66] Copyright 2021, Elsevier. d) Protective mechanism and transformation process of fibroin molecules immobilized on a Li metal anode. e) Top-view and cross-sectional view SEM images of a deposited Li metal anode and Cryo-EM images of fibroin-added SEI layers on Li metal. f) ATR-FT-IR spectra of pristine fibroin and recovered fibroin. g) Fluorescent image of fibroin

to further enhance the electrochemical performances of advanced batteries.

5. Proteins for Separators and Interlayers

The separators in rechargeable batteries play an essential role in isolating cathodes and anodes.[68,69] Meanwhile, they should also possess a good wettability toward electrolytes to ensure that the relevant metal ions can shuttle freely between the two electrodes. Moreover, since it may directly contact either of the electrodes, the separator material must be highly electrochemical stable to prevent it from participating in any redox reactions. With the development of high-energy-density batteries, especially for those with alkali metal anodes, the requirements for the separator are more stringent because any dendrite growing can easily penetrate through separators, resulting in short circuits and even thermal runaway of the battery. Therefore, the preparation of environmentally friendly and safe separators using proteins has emerged in the past few years.[70–75] The first application of protein-based separator was reported in 2018. Fu et al. reported a self-assembled protein nanofilter on a separator to trap polysulfides (**Figure 8**a).[70] The 3D porous structures of polysulfide nanofilters (PSNFs) were prepared via the self-assembling nature of the proteins (Figure 8b). The unique porous structure is generated due to the interaction among the gelatin–particles and the internal gelatin–gelatin interactions. The trapping of polysulfides is realized through the interaction between the functional groups of proteins and lithium polysulfides as evidenced by the molecular dynamic simulations. Figure 8c shows the adsorption process of polysulfides (e.g., Li_2S_4) onto gelatin, during which the polysulfide molecules can be anchored onto the protein surface more or less instantaneously. Moreover, the "molecular cages" derived from unique spatial structures of protein chains may accommodate the dissolved polysulfides, thus increasing the adsorption capacity. The cycling performance of the Li–S cells with PSNF-coated separators showed significantly improved capacity retention (75% of the initial capacity) compared with cells with only the pristine separator (65% of the initial capacity). SEM images of PSNF before and after cycling show all the pores are filled with polysulfides, demonstrating the excellent adsorption ability of the as-prepared protein-coated separator (Figure 8d).

Later, Nie et al. also employed bio-nanofiber coated separators to suppress the growth of Li dendrite.[71] Figure 8e illustrates the configuration of a Li-ion battery with a CsgA-modified separator, in which the CsgA modification glues the separators and electrodes like a "zipper," pulling them tightly together in the liquid electrolyte. As shown in Figure 8f, the biofilm nanofiber-coated separator marked by CdSeS@ZnS quantum dots emitted strong and homogeneous red fluorescence, demonstrating that the CsgA coating layer is uniform. The CsgA modification also improves the wettability of the separator for the electrolyte (Figure 8g). When applied in Li||Li symmetric cells, the modified separator delivered an alleviated polarization and prolonged cycling life compared to the pristine separators at 1.0 mA cm^{-2} for a plating/stripping capacity limitation of 1.0 mAh cm^{-2}. The improved electrochemical performance of the cells was contributed by the close contact between the electrodes and separators derived from the protein modification. In 2020, Chen et al. reported a "Janus" protein-based nanofabric for alleviating the growth of Li dendrites and trapping polysulfides to inhibit the "shuttle effect" (Figure 8h).[72] The Janus nanofabric is composed of two different layers. One layer is a gelatin-coated conductive CNF for absorbing lithium polysulfide, and the other layer is an insulative gelatin nanofabric for regulating Li metal deposition. When applying the "Janus" separator into Li||Li symmetric cells, the average voltage polarization during the plating/stripping process was significantly reduced compared with the cells using commercial Celgard separators, confirming the excellent ionic conductivity of the gelatin-nanofabric (Figure 8i). After 26 cycles, the retrieved Li metal anodes with gelatin-nanofabric showed smooth and homogeneous morphology. Moreover, Li–S batteries using "Janus" nanofabric separator consistently demonstrated high reversible capacities at different current densities.

Chen et al. used two types of proteins, gelatin and zein, composited with carbon nanofibers to modify separators for Li–S batteries, as illustrated in **Figure 9**a.[75] Both proteins were denatured in acidic solutions to break the H-bonds and salt bridges, resulting in the exposure of random polypeptide chains with different side groups (Figure 9b). The fabrication process continued by growing a thin coating layer of protein on the surface of carbon nanofibers (Figure 9c). For Li–S full cell testing, cells with three different interlayers, gelatin/CNF, zein/CNF, and poly(vinylpyrrolidone) /CNF, all exhibited much-improved discharge capacities and cycling stability. In particular, the cells with gelatin/CNF interlayers showed the best performance, with an initial discharge capacity of 1105 mAh g^{-1} at a current density of 0.3 A g^{-1}, and a capacity of 628 mAh g^{-1} being maintained after 250 cycles (Figure 9d). Experimental and theoretical calculation results verified that the lengths of the side chains of the denatured proteins play an essential role in trapping polysulfides. The gelatin protein consists of short-chain residues (e.g., glycine, proline) showed significantly stronger adsorption capability of polysulfides compared with zein which consists of many long-chain residues (e.g., glutamine, leucine). This work provides a strategy for the selection of protein molecules for polysulfide trapping.

Tao and co-workers modified natural eggshell membrane (ESM) as an interlayer to regulate Li deposition and suppress dendrite formation.[73] The ESM obtained by removing $CaCO_3$ from eggshells showed very good flexibility (Figure 9e). One-step 2,2,2-trifluoroethanol solvothermal treatment was used to stabilize the natural structure of the proteins. Significant

molecule distribution on defects of Li metal foil under UV light (characterized by two-photon confocal microscopy). h) Galvanostatic cycling of symmetric Li||Li cells with (blue line) or without (red line) a fibroin interlayer at 3 mA cm^{-2} with a capacity limitation of 1 mA cm^{-2}. i) Coulombic efficiencies of Li||Cu half cells with and without fibroin at 1 mA cm^{-2} and 1 mAh cm^{-2}. Reproduced with permission.[67] Copyright 2020, Springer Nature.

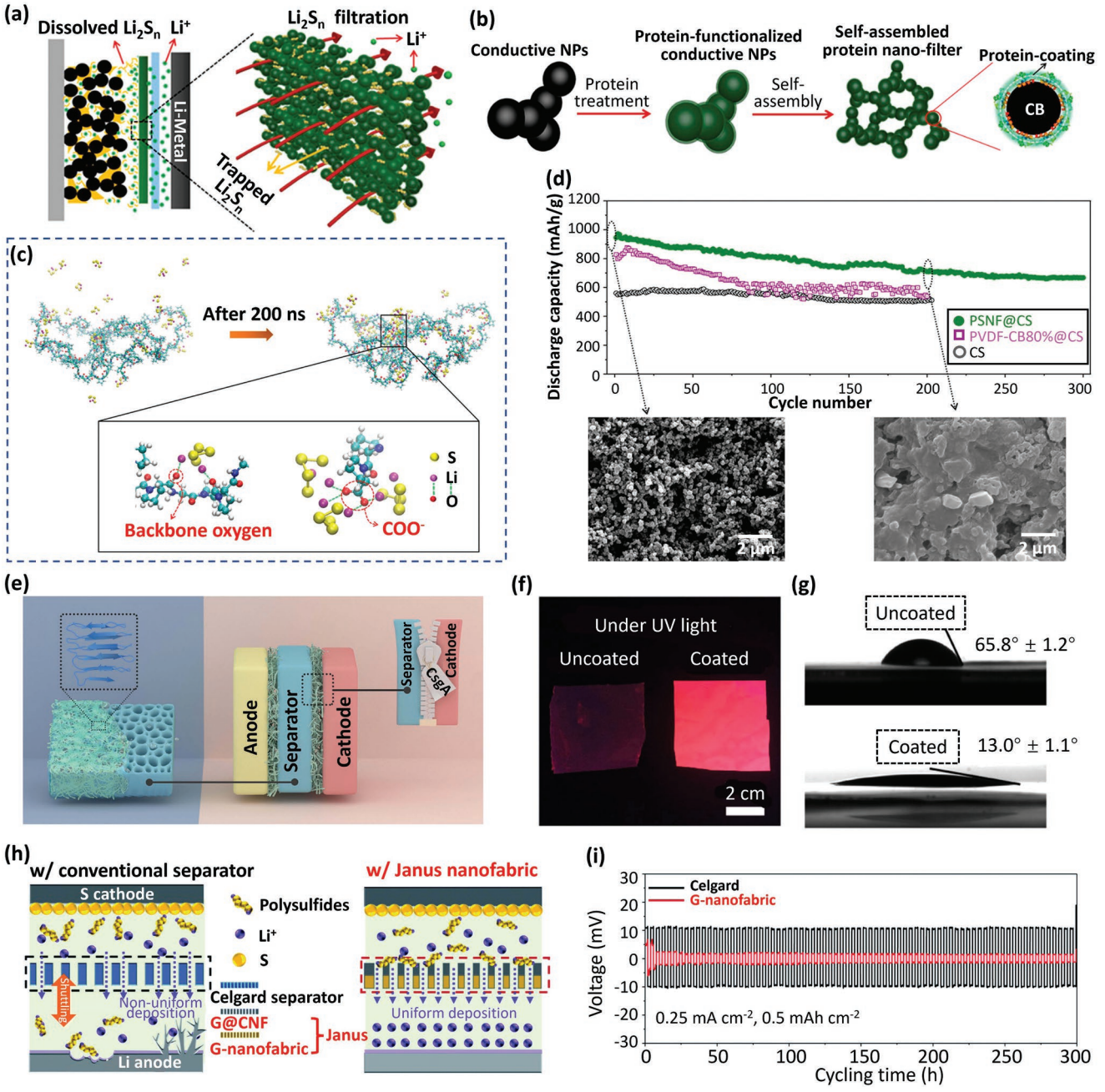

Figure 8. a) Illustration of a cell configuration with PSNF to stop the "shuttle effect" of polysulfides. b) Schematic diagram of the facile preparation process of the self-assembled protein nanofilter. c) Snapshots of Li_2S_4 and gelatin from initial and final states (after 200 ns) corresponding to interactions in liquid electrolyte. d) Cycling performance of the cells with different separators at 0.3 A g^{-1}, and the corresponding SEM images before and after 200 cycles. Reproduced with permission.[70] Copyright 2018, American Chemical Society. e) The working mechanism of the CsgA protein-modified separator in Li metal batteries. f) Digital photos of a pristine (left) and BN-coated separator (right) after incubating with CdSeS@ZnS QD solution under UV light. g) Electrolyte contact angle testing on pristine and coated separators. Reproduced with permission.[71] Copyright 2019, American Chemical Society. h) Schematic illustration of the working mechanism of "Janus" nanofabric to restrict polysulfide diffusion in Li–S cells. i) Voltage versus time profiles of Li||Li symmetric cells at 0.25 mA cm^{-2}, 0.5 mAh cm^{-2} with pristine and gelatin (G)-nanofabric coated separator. Reproduced with permission.[72] Copyright 2020, Royal Society of Chemistry.

Li deposition behaviors were observed on pristine Cu foil and TESM-covered Cu foil (Figure 9f,h). In the presence of the TESM interlayer, dendrite-free Li with spherical microstructure can be obtained, which should be contributed by the strong Li-ion affinity with the functional groups of proteins (Figure 9g). The authors also used Cryo-EM to confirm that the growth of Li dendrites (usually preferring the ⟨111⟩ crystallographic orientation) was significantly suppressed in the presence of the protein. In addition, the naturally soluble chemical species from protein also participated in the formation of SEI.

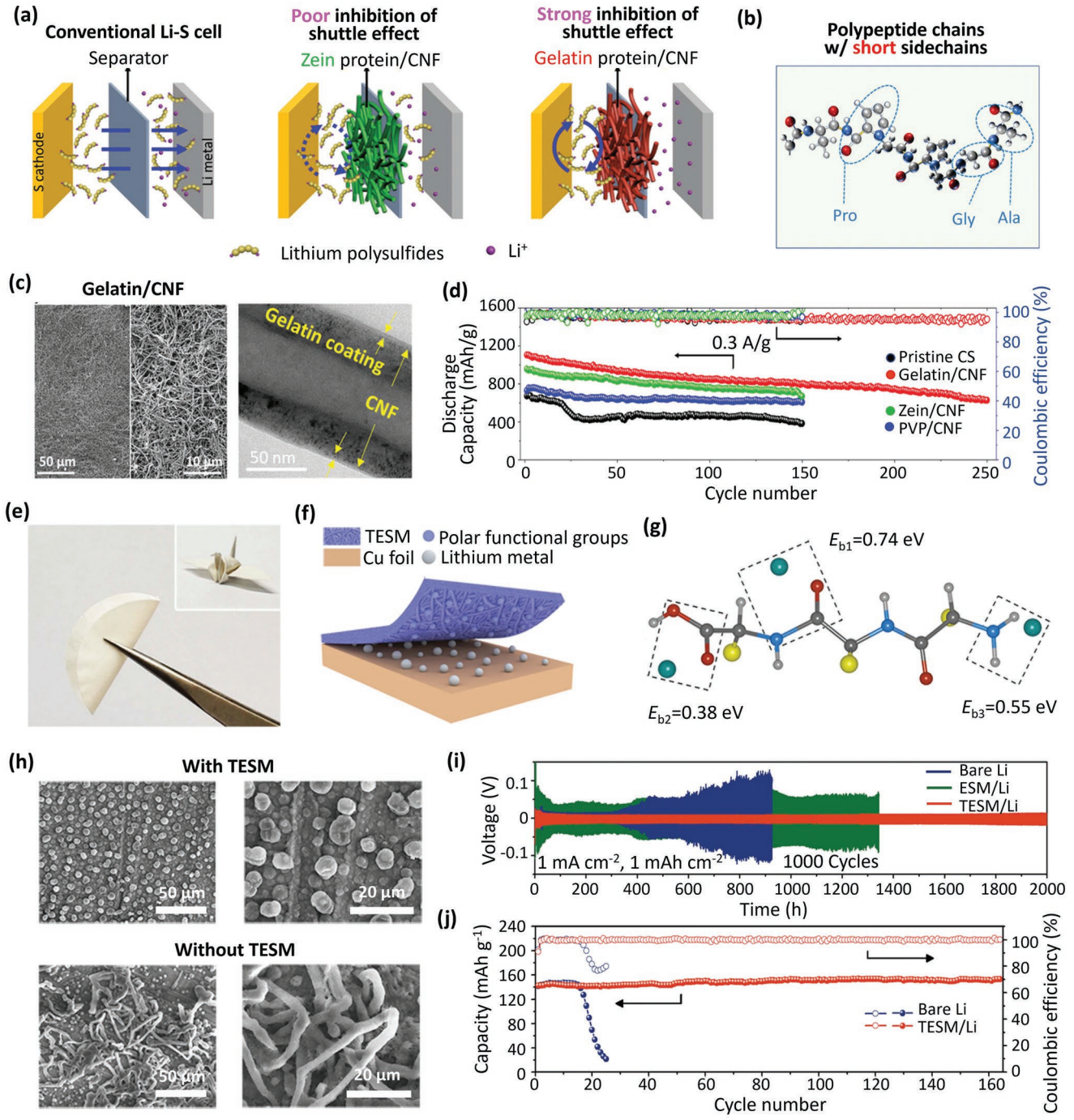

Figure 9. a) Schematic illustration of the design strategy to use protein-based interlayers for trapping polysulfides in Li–S batteries. b) Illustration of molecular structure of denatured gelatin proteins with short-chain residues. c) SEM and TEM images of gelatin/CNF nanocomposite. d) Cycling stability of Li–S cells with different interlayers at 0.3 A g^{-1}. Reproduced with permission.[75] Copyright 2020, Wiley-VCH. e) Digital photos of bent and folded eggshell membranes (ESM). f) Illustration of Li growth on TESM-modified Cu foil. g) Illustration of the strong interactions between Li^+ ions and polar groups within TESM. h) SEM images of Li deposition on Cu foils with and without TESM. i) Cycling performance of Li||Li symmetric cells with and without interlayer. j) Cycling performance of Li||$LiFePO_4$ full cells with pristine and TESM protected Li metal anodes. Reproduced with permission.[73] Copyright 2020, Springer Nature.

This effectively modified the physicochemical properties of SEI, which facilitated uniform Li deposition. When cycled at 1 mA cm^{-2} for 1 mAh cm^{-2}, Li||Li symmetric cells with ESM interlayers maintained a low polarization up to 2000 h, which is much longer than the cells without the interlayer (Figure 9i). The Li||$LiFePO_4$ full cell with ESM interlayer on Li anodes also exhibited eight times longer cycle life than the cells with pristine Li anodes (Figure 9j).

6. Proteins as Artificial Protective Films

Constructing artificial protective films on the surface of alkali metal anodes has been demonstrated to be an effective method to improve the stability of electrolyte/electrode interfaces.[76–81] Proteins have also been used to construct artificial protective films on Li metal anodes to facilitate uniform Li deposition and suppress dendrite formation. As an example, Wu et al. used a sericin protein to fabricate a conformal protective coating layer on Li metal anodes.[82] Due to the abundant lithiophilic and anionic functional groups on the polypeptide chain of sericin protein, the Li-ion transference number near the surface of Li metal anodes was significantly increased to 0.876 after surface coating. As a result, uniform Li deposition behavior in an island-like or lateral growth mode at the electrode/electrolyte interface has been observed. Sericin-decorated Li||Cu half cell exhibited long cycle life (335 cycles) and high Coulombic efficiency (98%). Even at an extremely high current density of 10 mA cm^{-2} with the capacity limitation of 5 mAh cm^{-2}, the sericin-decorated Li metal anode still maintained excellent cycling stability (160 cycles). The sericin-based protective layer also greatly improved the stability of Li metal even in the normal atmosphere.

Besides sericin, other proteins with similar properties can also be used as artificial protective layers to stabilize Li metal electrodes. To enhance the mechanical properties of the protein membranes to tolerate large stresses of volume expansion and contraction during alkali metal plating/stripping process, mixing proteins with other polymer materials has been investigated. Wang et al. prepared a composited artificial SEI consisting of denatured zein protein and polyethylene oxide (PEO) (**Figure 10**a,b).[83] Pure zein films showed many cracks after the removal of solvents, driven by their strong inter-/intrachain interactions (Figure 10b). With the addition of PEO, the denatured protein chains were kept unfolded through intermolecular interactions with PEO polymers, thereby forming a uniform, highly flexible, and strong adhesive protective film on Li metal anodes. Conformal zein@PEO films offered strong anionic anchoring capability that enabled a high Li-ion transference number (0.80) (Figure 10c). Repeated Li plating/stripping tests with zein@PEO protective films showed that Coulombic efficiencies of Li||Cu half cells demonstrated the best performances at a range of current densities (Figure 10d). In combination with $LiMn_2O_4$ cathodes, the cycling stability and rate performances of full cells have been significantly

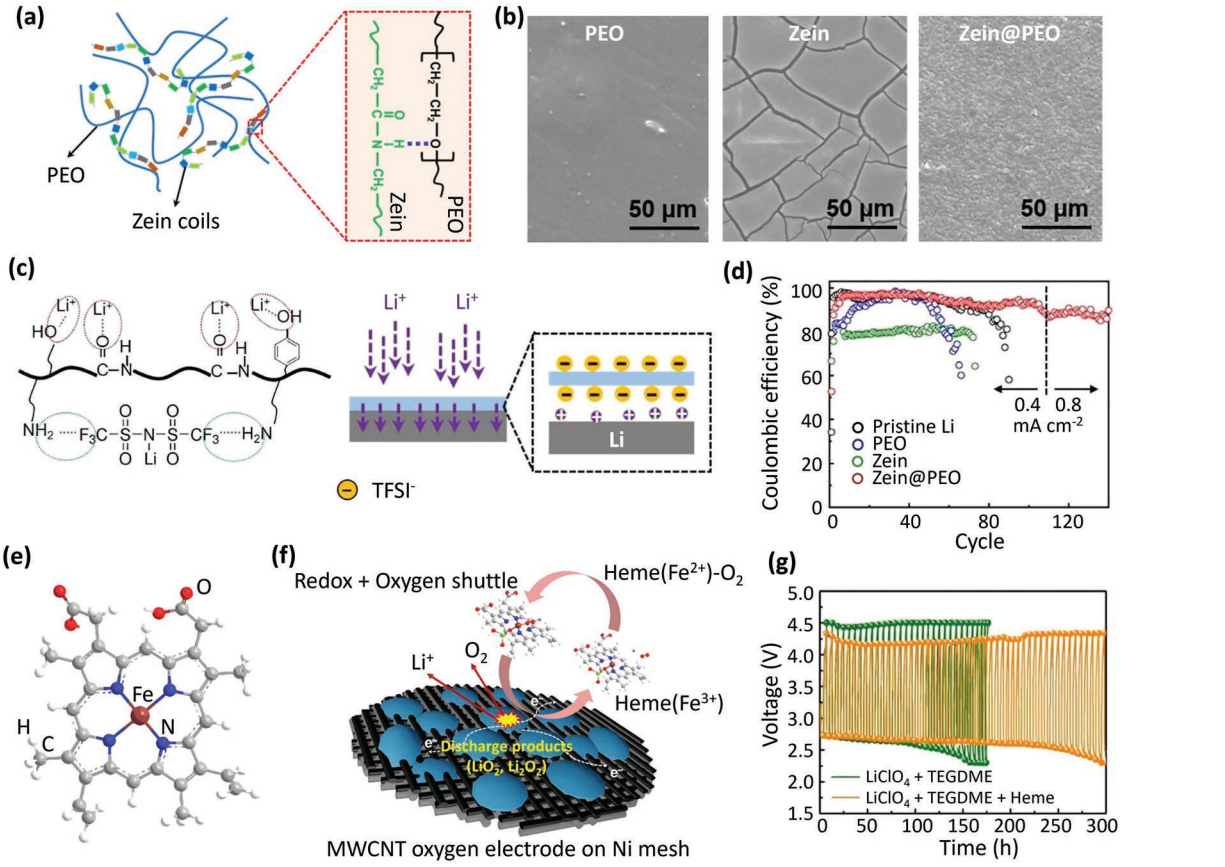

Figure 10. a) Schematic illustration of the formation of H-bonds between zein and PEO molecules. b) Morphologies of PEO, zein, and zein@PEO films formed in situ on Li metal anodes. c) Schematic of the contribution of zein to anchoring anions and then stabilizing ion deposition. d) Coulombic efficiencies of Li||Cu half cells with different protective films on Li metal anodes at current densities of 0.4 mA cm^{-2} and 0.8 mA cm^{-2}. Reproduced with permission.[83] Copyright 2008, Elsevier. e) Illustration of the heme molecular structure. f) Illustration of the reaction mechanism of heme as a redox mediator during the charge process in Li–O_2 batteries. g) Cycling performance of Li–O_2 batteries with and without heme in the electrolyte. Reproduced with permission.[85] Copyright 2016, Springer Nature.

improved, demonstrating the effectiveness of introducing zein@PEO protective films on Li metal anodes. Later, Akhtar et al. reported a simple bifunctional interlayer of gelatin-based fibers (GFs) to protect lithium anode surfaces from dendrite growth and prevent parasitic reactions with polysulfides.[84] The 3D structural network of GFs layers with abundant polar sites facilitates homogenized Li-ion flux, resulting in a uniform Li deposition. Simultaneously, the polar moieties also immobilize lithium polysulfides, protecting lithium metal from parasitic reactions.

7. Proteins as Catalysts

To expand the applications of biomaterials in energy storage devices, some proteins have been used as electrocatalysts to improve the electrochemical performances of rechargeable batteries. Ryu et al. reported the application of heme, a porphyrin cofactor in blood, as a biocatalyst in Li–O_2 batteries.[85] To overcome the electron transfer issue of traditional solid-state electrocatalysts, some soluble catalysts or redox mediators have been applied in Li–O_2 batteries to facilitate the decomposition of electronically insulating discharge products (e.g., Li_2O_2) during the charge process.[86–94] It has been shown that heme molecules 1 M $LiClO_4$ in tetraethylene glycol dimethyl ether electrolytes can function as a soluble redox catalyst and oxygen shuttle agent for efficient oxygen evolution reaction in Li–O_2 batteries. As illustrated in Figure 10e, the reversible chemical and electrochemical redox center is the rapid electron transfer to/from Fe ions (Fe^{3+}/Fe^{2+} couple) in heme. The unique molecular structure of the Fe ion center bonded with four pyrrole nitrogen leaves an open axial coordination site for dioxygen binding. Hence, heme can be used as a bifunctional redox mediator with charge transfer and oxygen-shuttling properties to reduce the charge overpotential of Li–O_2 batteries (Figure 10b). When tested at a current density of 100 mA g^{-1} carbon, the discharge capacities of the Li–O_2 cells with and without heme in the electrolytes are similar, but the cell using the heme shows a much lower average charge overpotential. When limited to a charge/discharge capacity of 600 mAh g^{-1}, Li–O_2 cells with heme additive showed greatly improved cycling stability (Figure 10g). Later, Lee et al. directly applied hemoglobin proteins as a catalytic electrode component to improve the electrochemical performance of Li–CO_2 batteries.[95] The hemoglobin proteins were combined with multiwall carbon nanotube at two different weight ratios to prepare porous cathodes. The authors discovered that Li–CO_2 cells containing hemoglobin catalysts obtained higher discharge/charge capacities due to the catalytic effect of hemoglobin for CO_2 reduction and oxidation, and optimized weight ratios between the protein and conductive carbon is essential to obtain the best performance. The authors also claimed that the redox reaction of Fe ion in the hemoglobin is responsible for CO_2 reduction and Li_2CO_3 oxidation.

The application of proteins as catalysts in advanced rechargeable batteries is still at an infant stage. The catalytic mechanism needs further investigation. Compared with traditional noble metal catalysts, the catalytic efficiency and stability of protein-based catalysts are still insufficient. However, the research on protein-based catalysts could be of great significance for the future development of microbatteries in medical and biological fields.

8. Proteins as Binders

Binder is one of the essential components in the preparation of porous electrodes in rechargeable alkali-ion batteries. Developing water soluble and environmentally friendly protein-based binders has attracted significant attention recently (**Table 2**). The binders directly from pristine proteins (e.g., gelatin, silk fibroin, casein, sericin) or protein-based composites have shown great potential to replace the traditional polymer binders such as PVDF for high-energy batteries. They have been used to prepare electrodes to enhance the integrity of electrodes against large volume change during the charge/discharge process and restrict the "shuttle effect" from the intermediates generated during the electrochemical reactions.

Gelatin has been successfully used as the binder to prepare high-performance sulfur cathodes in Li–S batteries.[96] The SEM images of the sulfur cathodes in **Figure 11**a show that sulfur and acetylene carbon black particles are well distributed in "SGA" electrodes (63 wt% sulfur + 7 wt% gelatin + 30 wt% acetylene black) before and after cycling. By contrast, many agglomerations were observed in "SPA" electrodes (i.e., 63 wt% sulfur + 7 wt% PEO + 30 wt% acetylene black) after cycling. Electrochemical impedance spectroscopy testing showed that the "SGA" electrodes demonstrate much lower charge-transfer resistance than "SPA" electrodes in 1 M $LiClO_4$ in dimethoxy ethane (DME)/1,3-dioxolane (DOL) ($V/V = 1/1$) electrolyte. The significantly improved electrochemical performance of the "SGA" electrodes compared with that of the "SPA" electrodes demonstrated that gelatin materials can be used as binders to improve the cycling stability of the sulfur cathodes in Li–S batteries.

Cheap and commercial-available silk fibroin proteins have also been widely employed as a natural binder for electrode preparation. Among all silk fibroin proteins, spider silk has been widely studied because of its unique physicochemical properties, such as semiamorphous layered structure with close stacked protein blocks, appropriate viscosity, and strong adhesion property. In 2020, Choi and Choy employed spider silk as the binder to prolong the cycling stability of silicon anodes in Li-ion batteries.[97] Benefiting from the excellent mechanical properties of silk fibroin, the electrode using this binder can effectively confine the nanosilicon particles in the electrode during the lithiation/delithiation process, similar to the working mechanism of the spider web. Compared to the electrodes prepared by PVDF binder, the silicon anodes containing spider silk binder achieved greatly enhanced discharge/charge specific capacities of 3642/1938 mAh g^{-1} in the 1st cycle and 1142/1054 mAh g^{-1} at the 5th cycle, respectively.

Using small protein molecules (e.g., casein) as binders has been found to be an effective strategy to improve the electrochemical performance of silicon anodes in Li-ion batteries.[98] The amine groups and carboxylic acid groups of casein can form abundant bonds with the silanol groups formed by silicon during the electrode preparation process (Figure 11b).

Table 2. Comparison of different proteins as binders in various rechargeable batteries.

Binders	Applications	Electrode	Electrolyte	Electrochemical performances	Refs.
Gelatin	Sulfur cathode in Li–S battery	63 wt% sulfur + 7 wt% binder + 30 wt% acetylene black	1 M $LiClO_4$ in DME/DOL	408 mAh g^{-1} at 0.4 mA cm^{-2} after 50 cycles	Ref. [96]
Silk fibroin	Silicon anode in Li-ion battery	45 wt% silicon + 10 wt% binder + 45 wt% carbon black	1 M $LiPF_6$ in EC/DEC	333 mAh g^{-1} at 250 mA g^{-1} after 38 cycles	Ref. [97]
Casein	Silicon anode in Li-ion battery	50 wt% silicon + 25 wt% binder + 25 wt% carbon black	1.2 M $LiPF_6$ in EC/DEC/FEC	1000 mAh g^{-1} at after 200 cycles	Ref. [98]
Sericin	LNMO cathode in Li-ion battery	80 wt% LNMO + 10 wt% binder + 10 wt% acetylene black	1 M $LiPF_6$ in EC/DEC	105.8 mAh g^{-1} at 140 mA g^{-1} after 100 cycles	Ref. [99]
P-SPI/PA/GG	Sulfur cathode in Li–S battery	90 wt% S/3D carbon + 10 wt% binder	LiTFSI in DOL/DME + 2 wt% $LiNO_3$	616.7 mAh g^{-1} at 1675 mA g^{-1} after 700 cycles	Ref. [100]
P-SPI/PEO/PA	Sulfur cathode in Li–S battery	90 wt% S/3D carbon + 10 wt% binder	LiTFSI in DOL/DME + 2 wt% $LiNO_3$	629.7 mAh g^{-1} at 1675 mA g^{-1} after 800 cycles	Ref. [101]
SPI–PAM	Sulfur cathode in Li–S battery	90 wt% S/3D carbon + 10 wt% binder	LiTFSI in DOL/DME + 2 wt% $LiNO_3$	677.6 mAh g^{-1} at 1675 mA g^{-1} after 350 cycles	Ref. [102]
SP/PAA	Sulfur cathode in Li–S battery	67.5 wt% sulfur + 10 wt% binder + 22.5 wt% carbon black	LiTFSI in DOL/DME + 2 wt% $LiNO_3$	600 mAh g^{-1} at 500 mA g^{-1} after 200 cycles	Ref. [103]
SP/PA	Sulfur cathode in Li–S battery	70 wt% sulfur + 10 wt% binder + 20 wt% carbon black	LiTFSI in DOL/DME + 1 wt% $LiNO_3$	803 mAh g^{-1} at ≈335 mA g^{-1} after 100 cycles	Ref. [104]

Four different electrodes were evaluated with different binders, including casein, PVDF, casein glue, and casein–PVDF (Figure 11c). The galvanostatic charge/discharge tests of both Si||Li half cells and $LiCoO_2$||Si full cells showed that using the casein binder can significantly improve their cycling performances (Figure 11d).

The choice of binders has been found to be an important factor that influences the formation of SEI or CEI on electrode materials.[105–107] An ideal situation during the electrode preparation process is that the electrode materials can be fully covered by a thin layer of binder materials.[99] The homogeneous coverage of binders on the electrode materials could provide high ionic conductivity and facilitate the formation of a stable and homogenous SEI/CEI. Especially for 5.0 V high-voltage electrodes in Li-ion batteries, such as $LiNi_{0.5}Mn_{1.5}O_4$ (LNMO) cathodes, the continuous oxidation of electrolytes could be avoided if the electrode materials and electrolytes were separated by a homogeneous binder layer and SEI layer as reported by Tang et al. (Figure 11e).[99] The electrolyte oxidation can be effectively suppressed by the introduction of electrochemically stable sericin as the binder. Sericin has a high solubility in an aqueous environment, which is attributed to its many polar side groups (e.g., glycine, threonine, and serine). During the electrode preparation process in the aqueous mixed slurry, sericin can be homogeneously coated on the surface of the cathode materials, which improves the interfacial stability of the electrode materials at high charging voltages. The self-discharge tests (i.e., voltage decay as a function of time under resting conditions) were conducted after charging the LNMO cathodes to 4.95 V.[99] The LNMO electrodes with sericin binder showed very small voltage decay after resting for more than 150 h (Figure 11f). By contrast, the voltage of the LNMO electrodes with PVDF binder quickly decreased after resting for 25 h. In addition, with the increasing weight ratio of sericin in the LNMO electrodes, the voltage stability under resting conditions can be further improved (Figure 11g), demonstrating that the good coverage of the LNMO particles with stable protein materials is an essential factor to prohibit parasitic reactions such as electrolyte decomposition.

To overcome some drawbacks of using single protein as binders, a biopolymer network combining different proteins has been explored by Wang et al.[100] The binder consists of guar gum (GG), phytic acid (PA), and SPI. In the designed binder, GG can restrict the volumetric expansion of sulfur cathodes; PA acts as a physical crosslink agent; SPI is used to anchor polysulfides (**Figure 12**a). In addition, the composite binder produced by blending the crosslinking showed superior mechanical properties that greatly improved the electrochemical performances of sulfur cathodes in Li–S batteries. As shown in Figure 12b, cells based on composite binder (P-SPI/PA/GG, PPG) showed the highest specific capacity of 773 mAh g^{-1} at 1 C among all the cells trailed with different binders for comparison. After 700 cycles, the Li–S battery can still maintain a capacity of 616 mAh g^{-1} with a capacity loss of only 0.029% per cycle. Wang et al. also investigated water-based phytic acid crosslinked supramolecular binders in Li–S batteries.[101] The binder consists of phosphorylated soybean protein isolate (P-SPI), PEO, and PA, which is denoted as SPP. The strong physical crosslinking of PA with the abundant amide groups and phosphate groups could decrease or even prevent

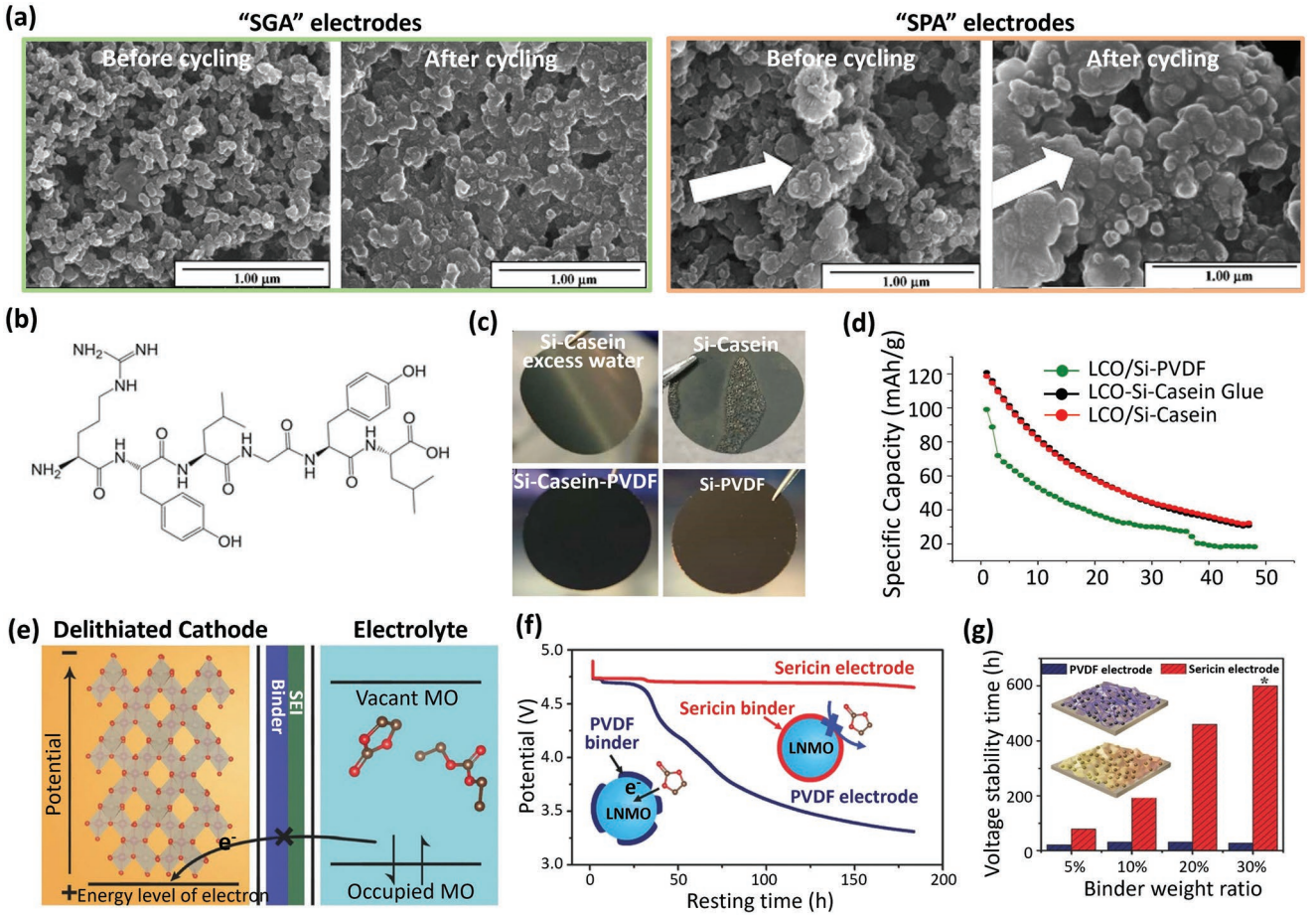

Figure 11. a) SEM images of the "SGA" electrodes and "SPA" electrodes before cycling and after cycling. Reproduced with permission.[96] Copyright 2008, Elsevier. b) Molecular structure of casein protein. c) Digital photos of the as-prepared electrodes with different binders. d) Cycling performance of $LiCoO_2$||Si full cells with different binders. Reproduced with permission.[98] Copyright 2019, The Electrochemical Society. e) Schematic illustration of an ideal SEI/binder system for the electrochemical stability of electrolyte molecular orbitals (MO) in the delithiated state. f) Self-discharge testing of high-voltage Li-ion batteries with different binders. g) Self-discharge testing of high-voltage Li-ion batteries with different weight ratio of binders in the electrodes. Reproduced with permission.[99] Copyright 2017, Wiley-VCH.

the dissolution of PEO in the electrolyte. When applied to Li–S batteries, the cell using SPP binder supported a discharge capacity of 932 mAh g^{-1} at 0.1 C, even at a high sulfur loading of 8.9 mg cm^{-2}. After 800 cycles, a capacity of 629 mAh g^{-1} can be maintained, with a low-capacity attenuation of only 0.0298% per cycle.

In order to further exploit the potential of soybean protein as a natural binder in Li–S batteries, Wang et al. combined SPI with PAM to improve the mechanical strength and bonding properties of biomaterial-based binders.[102] The addition of PAM can largely improve the physiochemical properties of the SPI binder, endowing it with excellent adhesion and good self-healing capability (Figure 12c). When used in the preparation of sulfur cathodes, the SPI–PAM binder exhibited strong lithium polysulfide trapping capability that enabled significantly improved cycling stability of Li–S batteries with high sulfur-loaded cathodes. The sulfur cathodes prepared by SPI–PAM binder showed the highest initial discharge capacity and best cycling stability compared with that prepared by SPI, PAM, and PVDF binder (Figure 12d). For high-rate performance tests, the sulfur cathodes with SPI–PAM binder could also be cycled up to a current rate of 20 C. Except for PAM, other polymers were also used to strengthen the mechanical properties of soybean protein. Fu et al. incorporated soy protein (SP) with poly(acrylic acid) (PAA) to obtain an SP-based binder with multiple functionalities and high mechanical robustness (Figure 12e).[103] SP can provide excellent Li-ion conductivity near the surface of the electrode materials, and the addition of PAA enables a robust conduction network. In addition, the abundant amino acid groups of SP provide strong binding to lithium polysulfides. The Li–S batteries with SP–PAA binder delivered improved charge/discharge capacity and cycling stabilities at different current densities compared with pristine SP, PAA, and commercial PVDF binders (Figure 12f).

To further integrate more functions of protein-based binders, Qui et al. reported an aqueous supramolecular binder combining PA and crosslinked SP for Li–S batteries with excellent flame retardant properties to improve the safety of high-energy batteries.[104,108,109] The combination of PA and SP allows the binder to trap lithium polysulfides via electrostatic interactions, alleviating the volume change of the sulfur cathode during lithiation and delithiation processes, and providing excellent flame

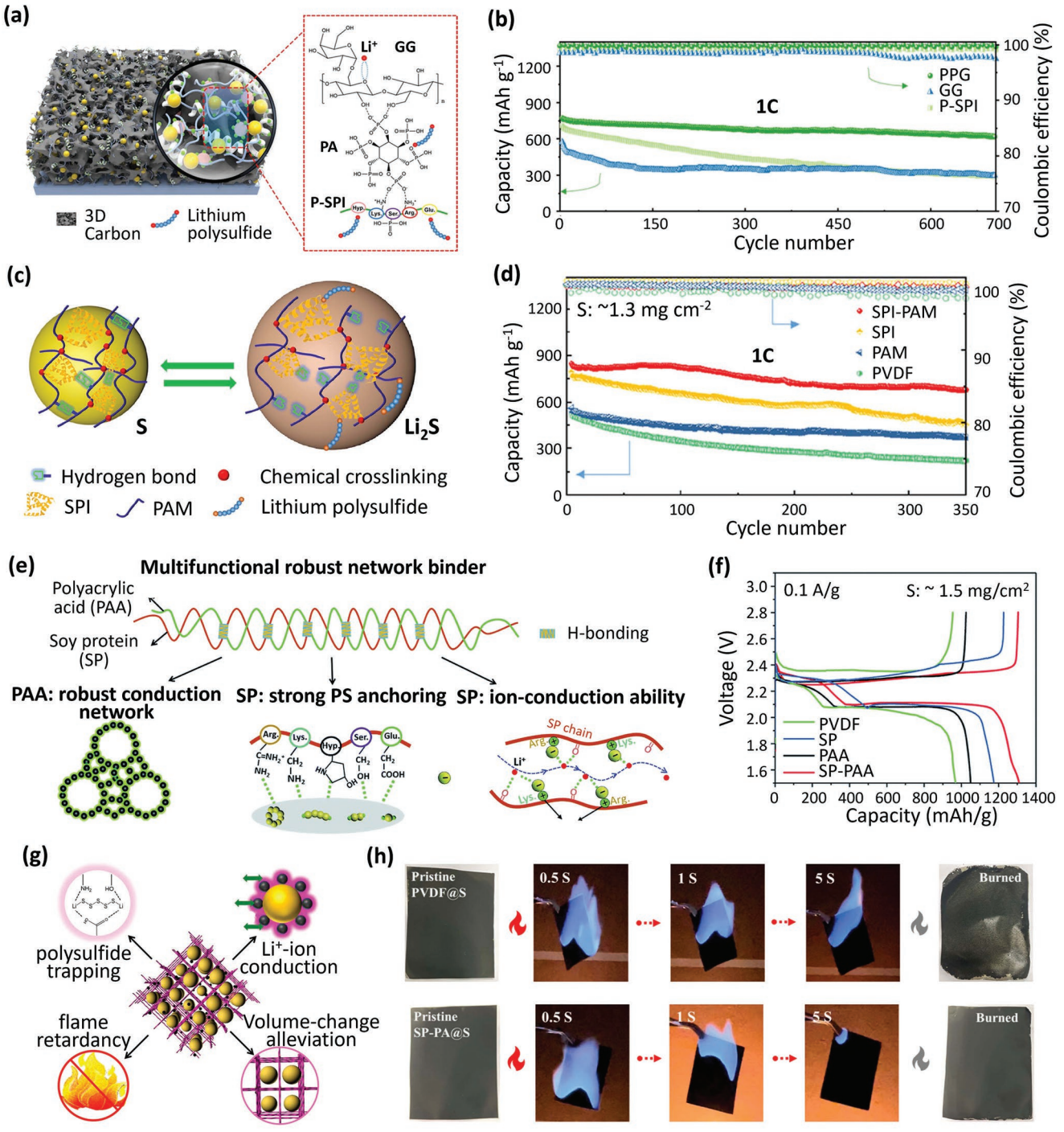

Figure 12. a) Schematic illustration of a sulfur electrode with P-SPI–PA–GG (PPG) binder to trap lithium polysulfides. b) The cycling performances of Li–S batteries using different binders at a current rate of 1 C. (Phosphorylated soybean protein, P-SPI; phytic acid, PA; guar gum, GG.) Reproduced with permission.[100] Copyright 2020, American Chemical Society. c) Schematic illustration of the self-healing mechanism of SPI–PAM binder in a sulfur cathode during lithiation and delithiation processes. d) Cycling performance of Li–S batteries with different binders at a current rate of 1 C with the sulfur loading of ≈1.3 mg cm^{-2}. Reproduced with permission.[102] Copyright 2020, American Chemical Society. e) Schematic illustration of the advantages of the multifunctional SP–PAA binder. f) Typical charge–discharge voltage profiles of sulfur cathodes with different binders. Reproduced with permission.[103] Copyright 2019, Royal Society of Chemistry. g) Schematic illustration of the multifunctional SP–PA binder. f) Flame-retardance SPI tests of sulfur cathodes with PVDF and SP–PA binders. Reproduced with permission.[104] Copyright 2021, American Chemical Society.

retardancy properties (Figure 12g). The flame-retardance test results showed that the burning time of sulfur cathodes was significantly reduced when using the SP–PA binder compared with the cathodes using SP and PVDF binders (Figure 12h). Two mechanisms were used to explain the SP–PA flame retardancy. i) The decomposition of PA instantaneously releases

phosphoric acid/water gas, which forms an isolating layer that stops the heat and oxygen diffusion. Meanwhile, some noncombustible gases (e.g., CO_2 and N_2) released from the decomposition of SP can dilute the combustible gas concentration and absorb heat energy. ii) During the PA thermal decomposition, numerous PO$^{\bullet}$ radicals can capture $^{\bullet}$OH and H$^{\bullet}$ radicals, which restricts further chain reactions. The cycling performances of sulfur cathodes with different binders were also tested at 0.2 C, and the PA–SP binder improved both the discharge capacity and cycling stability of the sulfur cathodes. SEM images of cycled sulfur cathodes with SP–PA binder show electrode surfaces still flat without obvious cracks, confirming that SP–PA binder can firmly bind the active materials together even under large volume expansion/contraction during cycling.

In summary, proteins as binders show several advantages. i) High ionic conductivity. ii) Low processing cost benefiting from abundant natural resources. iii) Environmental friendliness during the electrode manufacturing process. The use of water-soluble protein binders obviates the use of toxic organic solvents (e.g., *N*-methyl-2-pyrrolidone). iv) Owing to the abundant functional groups of protein molecules, protein-based binders exhibit excellent capability for trapping polysulfides to suppress the "shuttle effect" in Li–S batteries. v) Protein-based composite binders with flame-retardant properties can effectively improve the safety of batteries.

9. Conclusion and Perspective

As an essential part of organisms, proteins have attracted tremendous interest due to their highly functional molecular structure and abundant chemical activities, endowing them with huge advantages beyond traditional artificial polymers. So far, the development of proteins used in different battery components has achieved considerable success.

As major components of the electrolytes, the utilization of proteins to replace toxic organic materials reduces cost and environmental impacts and improves the safety of rechargeable batteries. Besides these advantages, protein-based electrolytes also suppress parasitic reactions by reducing the reactivity of water molecules in aqueous batteries, improving the interface stability of the metal anodes, and expanding the electrochemical stability windows of rechargeable batteries. Several quasi-solid-state electrolytes prepared from proteins can reduce lithium polysulfide dissolution and suppress the detrimental "shuttle effect" in Li–S batteries. Furthermore, the ionic conductivity and mechanical strength of protein-based solid-state electrolytes can be further improved by cooperating with other polymers.

As electrolyte additives, proteins show many advantages beyond traditional polymer additives. Protein molecules can selectively and preferentially adhere to defects on the surfaces of metal anodes, which change the local electric field distribution and suppress dendrite growth. The unique secondary structure transformation of proteins in electrolytes enhances their adsorption effects. In addition, protein additives participate in the formation of SEI with enhanced mechanical properties and improved ionic conductivity. Those additives also selectively adsorb and repair the cracks of SEI during cycling, hence providing long-term protection for the metal anodes. As for the ex situ construction of artificial protective films on metal anodes, protein-based films also show enhanced mechanical strength, excellent flexibility, and high ionic conductivity. In situ formed SEI with electrolyte additives and artificial protective films have common points in several aspects but are significantly different. The artificial protective films are normally much thicker than the in situ formed SEI and show enhanced protection on reactive metal anodes from oxidation, even exposed to air. However, the artificial protective films from proteins may exfoliate from the substrate during cycling, resulting in a decrease in the protection ability.

Separators prepared from proteins show excellent ionic conductivities and wettability for both organic and aqueous electrolytes. They also have a higher polarity, which shows a stronger inhibitory effect on the polysulfide "shuttle effect" in Li–S batteries. As electrocatalysts, proteins containing metal ions act as redox mediators to improve the electrochemical performance of Li–O_2 batteries. Some proteins can also play a role in oxygen transmission, thus further enhancing the performance of Li–O_2 batteries.

The intensive application of proteins as binders demonstrates their great potential to replace the commonly used industry polymers in the preparation of electrodes. The appropriate viscosity of proteins can improve the dispersibility of active materials and prevent shrinking and cracking during the electrode preparation process. The excellent solubility of some proteins in aqueous solutions also overcomes the shortcomings of using toxic traditional organic solvents in the battery industry. In the field of Li–S batteries, the use of protein binders can also effectively inhibit the "shuttle effect" of polysulfides.

Meanwhile, the levels of protein structure show different influences on battery performances. The primary structure of proteins directly determines the chemical composition and functional groups. During the deposition process of alkali metal ions, proteins with different primary structures can directly affect the chemical composition of SEI on the surface of metal anodes, thus affecting the polarization, ionic conductivity, and electrochemical stability of SEI. The integration of some unreacted protein molecules may change Young's modulus and other mechanical properties of SEI. Functional groups containing heteroatoms such as S and N in proteins can immobilize the reaction intermediates and suppress the "shuttle effect" in Li–S batteries. Moreover, some functional groups of proteins can complicate with multivalent ions, thus acting as carriers, which is beneficial to the deposition and migration of multivalent ions.

The secondary structure of proteins mainly determines the status of protein in the electrolytes. Proteins often exist in the form of micelles in the electrolyte. Therefore, the transformation of protein secondary structure has a great impact on its dispersion in the electrolyte and the coverage of defects on the surfaces of electrodes. In organic electrolytes, proteins with β-sheet structure have higher solubility than that of α-helix structure due to the exposure of more hydrophobic functional groups. Proteins with β-sheet structure can induce more uniform transport of lithium ions, which has a positive significance for dendrite inhibition.

The study of tertiary structure of proteins is mainly limited to the catalytic field for metal–air batteries. Furthermore, the hydrogel formed by protein self-assembly plays an essential role in reducing the "shuttle effect" of undesired intermediates and improving the safety of rechargeable batteries. Unfortunately, the investigation of the quaternary structure of proteins in battery application lacks study yet. This is mainly due to the

tough environment inside the battery, which makes it difficult to stabilize the quaternary structure of proteins. However, we believe that with the rapid development of aqueous and biological batteries, the research on quaternary structure of proteins will achieve a quick development in the future.

Due to the excellent performance of proteins, it can be predicted that proteins will continue to add positive features to batteries into the future. Development of proteins in batteries may usefully focus on the following directions. i) It has been proved to be an effective method for preparing functional materials by mixing proteins with polymers. Proteins' rich functional groups are essential resources for grafting polymer groups. The synergistic effect of protein and traditional industrial materials can greatly improve the performance of the battery and reduce manufacturing costs and the probabilities of side reactions. ii) Proteins with simple structures and abundant recourses will be the main key avenues of protein research in the future. For example, soybean protein, bovine serum albumin, whey protein, and silk fibroin in plant protein/fabrications will play a more critical role in the future. iii) More recent and novel characterization methods in the biological field will be applied to energy storage research, such as Cryo-EM, circular dichroism spectroscopy, and two-photon confocal fluorescence microscopy, which will enable increased capability in the research field of energy storage. iv) The protection mechanisms of some protein molecules in battery environments will provide important inspiration and a theoretical basis for the design and development of intelligent biomimetic molecules in the future. In the field of energy, intelligent molecular design and preparation can play an important role in the coming decades. We believe that in the coming decades, the participation of biological materials such as proteins will vastly enhance the capability of energy storage and other aspects of the energy field.

Acknowledgements

T.W., D.H., and H.Y. contributed equally to this work. X.G., B.S., and G.W. would like to acknowledge the financial support from the Australian Research Council (ARC) through the ARC Discovery projects (DP200101249 and DP210101389) and the ARC Industry Transformation Research Hub (IH180100020). T.W. would like to acknowledge the financial support from Natural Science Foundation of China (No. 22102141). H.Y. would like to acknowledge the financial support from the "Young scientists lifting project" of Jiangsu Province, China (TJ-2022-072), Yangzhou Social Development Project (YZ2020065).

Open access publishing facilitated by University of Technology Sydney, as part of the Wiley - University of Technology Sydney agreement via the Council of Australian University Librarians.

Conflict of Interest

The authors declare no conflict of interest.

Keywords

batteries, biomaterials, electrochemistry, energy storage materials, proteins

Received: July 27, 2022
Revised: September 4, 2022
Published online: September 23, 2022

[1] S. Chu, A. Majumdar, *Nature* **2012**, *488*, 294.
[2] S. Chu, Y. Cui, N. Liu, *Nat. Mater.* **2017**, *16*, 16.
[3] I. Dincer, *Renewable Sustainable Energy Rev.* **2000**, *4*, 157.
[4] M. Armand, J.-M. Tarascon, *Nature* **2008**, *451*, 652.
[5] H. Chen, T. N. Cong, W. Yang, C. Tan, Y. Li, Y. Ding, *Prog. Nat. Sci.* **2009**, *19*, 291.
[6] S. Koohi-Fayegh, M. A. Rosen, *J. Energy Storage* **2020**, *27*, 101047.
[7] A. Poullikkas, *Renewable Sustainable Energy Rev.* **2013**, *27*, 778.
[8] B. Dunn, H. Kamath, J.-M. Tarascon, *Science* **2011**, *334*, 928.
[9] J. B. Goodenough, *Nat. Electron.* **2018**, *1*, 204.
[10] F. Wu, M. Liu, Y. Li, X. Feng, K. Zhang, Y. Bai, X. Wang, C. Wu, *Electrochem. Energy Rev.* **2021**, *4*, 382.
[11] N. S. Choi, Z. Chen, S. A. Freunberger, X. Ji, Y. K. Sun, K. Amine, G. Yushin, L. F. Nazar, J. Cho, P. G. Bruce, *Angew. Chem., Int. Ed.* **2012**, *51*, 9994.
[12] S. Zhang, S. Li, Y. Lu, *eScience* **2021**, *1*, 163.
[13] W. Yao, P. Zou, M. Wang, H. Zhan, F. Kang, C. Yang, *Electrochem. Energy Rev.* **2021**, *4*, 601.
[14] B. Sun, X. Huang, S. Chen, P. Munroe, G. Wang, *Nano Lett.* **2014**, *14*, 3145.
[15] B. Sun, P. Xiong, U. Maitra, D. Langsdorf, K. Yan, C. Wang, J. Janek, D. Schröder, G. Wang, *Adv. Mater.* **2020**, *32*, 1903891.
[16] K. Yan, J. Wang, S. Zhao, D. Zhou, B. Sun, Y. Cui, G. Wang, *Angew. Chem., Int. Ed.* **2019**, *58*, 11364.
[17] Z. Peng, S. A. Freunberger, Y. Chen, P. G. Bruce, *Science* **2012**, *337*, 563.
[18] Y. Yuan, R. Sharpe, K. He, C. Li, M. T. Saray, T. Liu, W. Yao, M. Cheng, H. Jin, S. Wang, *Nat. Sustain.* **2022**, https://doi.org/10.1038/s41893-022-00919-3.
[19] Z. Yi, J. Liu, S. Tan, Z. Sang, J. Mao, L. Yin, X. Liu, L. Wang, F. Hou, S. X. Dou, *Adv. Mater.* **2022**, *34*, 2203835.
[20] Y. Jin, P. M. Le, P. Gao, Y. Xu, B. Xiao, M. H. Engelhard, X. Cao, T. D. Vo, J. Hu, L. Zhong, *Nat. Energy* **2022**, *7*, 718.
[21] X. Fu, W. H. Zhong, *Adv. Energy Mater.* **2019**, *9*, 1901774.
[22] H. Yuan, T. Liu, Y. Liu, J. Nai, Y. Wang, W. Zhang, X. Tao, *Chem. Sci.* **2019**, *10*, 7484.
[23] C. Jin, J. Nai, O. Sheng, H. Yuan, W. Zhang, X. Tao, X. W. D. Lou, *Energy Environ. Sci.* **2021**, *14*, 1326.
[24] Q. Sun, B. Aguila, P. C. Lan, S. Ma, *Adv. Mater.* **2019**, *31*, 1900008.
[25] Z. Liu, P. Bertram, F. Endres, *J. Solid State Electrochem.* **2017**, *21*, 2021.
[26] Z. Li, F. Xu, C. Li, P. Wang, W. Yi, S. Wang, L. Yang, C. Yan, S. Li, *ACS Appl. Energy Mater.* **2021**, *4*, 1199.
[27] S. L. Baker, A. Munasinghe, B. Kaupbayeva, N. Rebecca Kang, M. Certiat, H. Murata, K. Matyjaszewski, P. Lin, C. M. Colina, A. J. Russell, *Nat. Commun.* **2019**, *10*, 4718.
[28] S. Liu, Z. Li, B. Yu, S. Wang, Y. Shen, H. Cong, *Adv. Colloid Interface Sci.* **2020**, *284*, 102254.
[29] X. Ge, D. S. C. Yang, K. Trabbic-Carlson, B. Kim, A. Chilkoti, C. D. M. Filipe, *J. Am. Chem. Soc.* **2005**, *127*, 11228.
[30] J. Britton, R. P. Dyer, S. Majumdar, C. L. Raston, G. A. Weiss, *Angew. Chem., Int. Ed.* **2017**, *56*, 2296.
[31] F. Shi, Q. Zhang, P. Wang, H. Sun, J. Wang, X. Rong, M. Chen, C. Ju, F. Reinhard, H. Chen, J. Wrachtrup, J. Wang, J. Du, *Science* **2015**, *347*, 1135.
[32] L.-G. Milroy, T. N. Grossmann, S. Hennig, L. Brunsveld, C. Ottmann, *Chem. Rev.* **2014**, *114*, 4695.
[33] K. A. Dill, J. L. MacCallum, *Science* **2012**, *338*, 1042.
[34] D. Kozakov, D. R. Hall, B. Xia, K. A. Porter, D. Padhorny, C. Yueh, D. Beglov, S. Vajda, *Nat. Protoc.* **2017**, *12*, 255.
[35] A. Drozdetskiy, C. Cole, J. Procter, G. J. Barton, *Nucleic Acids Res.* **2015**, *43*, W389.
[36] S. Wang, J. Peng, J. Ma, J. Xu, *Sci. Rep.* **2016**, *6*, 18962.
[37] H. Yang, S. Yang, J. Kong, A. Dong, S. Yu, *Nat. Protoc.* **2015**, *10*, 382.

[38] C. Louis-Jeune, M. A. Andrade-Navarro, C. Perez-Iratxeta, *Proteins: Struct., Funct., Bioinf.* **2012**, *80*, 374.
[39] A. Haim, S. Neubacher, T. N. Grossmann, *ChemBioChem* **2021**, *22*, 2672.
[40] F. A. Quiocho, *Annu. Rev. Biochem.* **1986**, *55*, 287.
[41] A. W. Senior, R. Evans, J. Jumper, J. Kirkpatrick, L. Sifre, T. Green, C. Qin, A. Zidek, A. W. R. Nelson, A. Bridgland, H. Penedones, S. Petersen, K. Simonyan, S. Crossan, P. Kohli, D. T. Jones, D. Silver, K. Kavukcuoglu, D. Hassabis, *Nature* **2020**, *577*, 706.
[42] N. Koga, R. Tatsumi-Koga, G. Liu, R. Xiao, T. B. Acton, G. T. Montelione, D. Baker, *Nature* **2012**, *491*, 222.
[43] K. Xu, *Chem. Rev.* **2004**, *104*, 4303.
[44] K. Xu, *Chem. Rev.* **2014**, *114*, 11503.
[45] W.-J. Chen, C.-X. Zhao, B.-Q. Li, Q. Jin, X.-Q. Zhang, T.-Q. Yuan, X. Zhang, Z. Jin, S. Kaskel, Q. Zhang, *Energy Environ. Mater.* **2020**, *3*, 160.
[46] S. Chai, Y. Zhang, Y. Wang, Q. He, S. Zhou, A. Pan, *eScience* **2022**, https://doi.org/10.1016/j.esci.2022.04.007.
[47] H. Li, C. Han, Y. Huang, Y. Huang, M. Zhu, Z. Pei, Q. Xue, Z. Wang, Z. Liu, Z. Tang, Y. Wang, F. Kang, B. Li, C. Zhi, *Energy Environ. Sci.* **2018**, *11*, 941.
[48] Q. Han, X. Chi, S. Zhang, Y. Liu, B. Zhou, J. Yang, Y. Liu, *J. Mater. Chem. A* **2018**, *6*, 23046.
[49] S. Zhang, N. Yu, S. Zeng, S. Zhou, M. Chen, J. Di, Q. Li, *J. Mater. Chem. A* **2018**, *6*, 12237.
[50] Q. Han, X. Chi, Y. Liu, L. Wang, Y. Du, Y. Ren, Y. Liu, *J. Mater. Chem. A* **2019**, *7*, 22287.
[51] C. Ding, L. Huang, Y. Guo, J.-l. Lan, Y. Yu, X. Fu, W.-H. Zhong, X. Yang, *Energy Storage Mater.* **2020**, *27*, 25.
[52] D. Zhou, L. Li, J. Du, M. Zhai, *Ionics* **2020**, *27*, 137.
[53] L. Shi, G. Wang, J. Li, M. Wu, Z. Wen, *ACS Sustainable Chem. Eng.* **2021**, *9*, 13883.
[54] K. Suvarnna, S. J. Kirubavathy, S. Selvasekarapandian, M. V. Krishna, M. Ramaswamy, *Ionics* **2022**, *28*, 1767.
[55] Y. Lu, T. Zhu, N. Xu, K. Huang, *ACS Appl. Energy Mater.* **2019**, *2*, 6904.
[56] H. McEvoy, S. B. Ross-Murphy, A. H. Clark, *Polymer* **1985**, *26*, 1483.
[57] D. A. Prystupa, A. M. Donald, *Polym. Gels Networks* **1996**, *4*, 87.
[58] X. Wang, G. Tan, Y. Bai, F. Wu, C. Wu, *Electrochem. Energy Rev.* **2021**, *4*, 35.
[59] S. Guo, L. Qin, T. Zhang, M. Zhou, J. Zhou, G. Fang, S. Liang, *Energy Storage Mater.* **2021**, *34*, 545.
[60] S. Li, W. Zhang, Q. Wu, L. Fan, X. Wang, X. Wang, Z. Shen, Y. He, Y. Lu, *Angew. Chem., Int. Ed.* **2020**, *59*, 14935.
[61] J. Han, Z. Chen, J. Xu, *Mater. Lett.* **2021**, *304*, 130629.
[62] B. Wang, R. Zheng, W. Yang, X. Han, C. Hou, Q. Zhang, Y. Li, K. Li, H. Wang, *Adv. Funct. Mater.* **2022**, *32*, 2112693.
[63] W. Gu, G. Xue, Q. Dong, R. Yi, Y. Mao, L. Zheng, H. Zhang, X. Fan, Y. Shen, L. Chen, *eScience* **2022**.
[64] J. Xu, W. Lv, W. Yang, Y. Jin, Q. Jin, B. Sun, Z. Zhang, T. Wang, L. Zheng, X. Shi, *ACS Nano* **2022**, *16*, 11392.
[65] C. Wang, X. Fu, C. Ying, J. Liu, W.-H. Zhong, *Chem. Eng. J.* **2022**, *437*, 135283.
[66] Y. Liu, Q. Shi, Y. Wu, Q. Wang, J. Huang, P. Chen, *Chem. Eng. J.* **2021**, *407*, 127189.
[67] T. Wang, Y. Li, J. Zhang, K. Yan, P. Jaumaux, J. Yang, C. Wang, D. Shanmukaraj, B. Sun, M. Armand, Y. Cui, G. Wang, *Nat. Commun.* **2020**, *11*, 5429.
[68] J. Zhang, B. Sun, X. Huang, S. Chen, G. Wang, *Sci. Rep.* **2014**, *4*, 6007.
[69] H. Hao, T. Hutter, B. L. Boyce, J. Watt, P. Liu, D. Mitlin, *Chem. Rev.* **2022**, *122*, 8053.
[70] X. Fu, C. Li, Y. Wang, L. Scudiero, J. Liu, W.-H. Zhong, *J. Phys. Chem. Lett.* **2018**, *9*, 2450.
[71] L. Nie, Y. Li, S. Chen, K. Li, Y. Huang, Y. Zhu, Z. Sun, J. Zhang, Y. He, M. Cui, S. Wei, F. Qiu, C. Zhong, W. Liu, *ACS Appl. Energy Mater.* **2019**, *11*, 32373.
[72] M. Chen, Z. Chen, X. Fu, W.-H. Zhong, *J. Mater. Chem. A* **2020**, *8*, 7377.
[73] Z. Ju, J. Nai, Y. Wang, T. Liu, J. Zheng, H. Yuan, O. Sheng, C. Jin, W. Zhang, Z. Jin, H. Tian, Y. Liu, X. Tao, *Nat. Commun.* **2020**, *11*, 488.
[74] Z. Ju, G. Lu, O. Sheng, H. Yuan, S. Zhou, T. Liu, Y. Liu, Y. Wang, J. Nai, W. Zhang, X. Tao, *Nano Lett.* **2022**, *22*, 1374.
[75] M. Chen, C. Li, X. Fu, W. Wei, X. Fan, A. Hattori, Z. Chen, J. Liu, W. H. Zhong, *Adv. Energy Mater.* **2020**, *10*, 1903642.
[76] L. Fan, B. Sun, K. Yan, P. Xiong, X. Guo, Z. Guo, N. Zhang, Y. Feng, K. Sun, G. Wang, *Adv. Energy Mater.* **2021**, *11*, 2102242.
[77] X. B. Cheng, R. Zhang, C. Z. Zhao, F. Wei, J. G. Zhang, Q. Zhang, *Adv. Sci.* **2016**, *3*, 1500213.
[78] R. Xu, X. Q. Zhang, X. B. Cheng, H. J. Peng, C. Z. Zhao, C. Yan, J. Q. Huang, *Adv. Funct. Mater.* **2018**, *28*, 1705838.
[79] K. Liu, A. Pei, H. R. Lee, B. Kong, N. Liu, D. Lin, Y. Liu, C. Liu, P.-c. Hsu, Z. Bao, *J. Am. Chem. Soc.* **2017**, *139*, 4815.
[80] A. C. Kozen, C.-F. Lin, A. J. Pearse, M. A. Schroeder, X. Han, L. Hu, S.-B. Lee, G. W. Rubloff, M. Noked, *ACS Nano* **2015**, *9*, 5884.
[81] Q. Wen, H. Fu, Z.-Y. Wang, Y. Huang, Z. He, C. Yan, J. Mao, X. Zhang, J. Zheng, *J. Mater. Chem. A* **2022**, *10*, 17501.
[82] H. Wu, Q. Wu, F. Chu, J. Hu, Y. Cui, C. Yin, C. Li, *J. Power Sources* **2019**, *419*, 72.
[83] C. Wang, X. Fu, S. Lin, J. Liu, W.-H. Zhong, *J. Energy Chem.* **2022**, *64*, 485.
[84] N. Akhtar, X. Sun, M. Y. Akram, F. Zaman, W. Wang, A. Wang, L. Chen, H. Zhang, Y. Guan, Y. Huang, *J. Energy Chem.* **2021**, *52*, 310.
[85] W. H. Ryu, F. S. Gittleson, J. M. Thomsen, J. Li, M. J. Schwab, G. W. Brudvig, A. D. Taylor, *Nat. Commun.* **2016**, *7*, 12925.
[86] Y. Chen, S. A. Freunberger, Z. Peng, O. Fontaine, P. G. Bruce, *Nat. Chem.* **2013**, *5*, 489.
[87] J. B. Park, S. H. Lee, H. G. Jung, D. Aurbach, Y. K. Sun, *Adv. Mater.* **2018**, *30*, 1704162.
[88] J. Zhang, Y. Zhao, B. Sun, Y. Xie, A. Tkacheva, F. Qiu, P. He, H. Zhou, K. Yan, X. Guo, *Sci. Adv.* **2022**, *8*, 1899.
[89] A. Tkacheva, B. Sun, J. Zhang, G. Wang, A. M. McDonagh, *J. Phys. Chem. C* **2021**, *125*, 2824.
[90] Z. Qian, X. Li, B. Sun, L. Du, Y. Wang, P. Zuo, G. Yin, J. Zhang, B. Sun, G. Wang, *J. Phys. Chem. Lett.* **2020**, *11*, 7028.
[91] A. Tkacheva, J. Zhang, B. Sun, D. Zhou, G. Wang, A. M. McDonagh, *J. Phys. Chem. C* **2020**, *124*, 5087.
[92] J. Zhang, B. Sun, Y. Zhao, A. Tkacheva, Z. Liu, K. Yan, X. Guo, A. M. McDonagh, D. Shanmukaraj, C. Wang, *Nat. Commun.* **2019**, *10*, 602.
[93] J. Zhang, B. Sun, Y. Zhao, K. Kretschmer, G. Wang, *Angew. Chem., Int. Ed.* **2017**, *56*, 8505.
[94] D. Cao, F. Yu, Y. Chen, X. Gao, *Energy Environ. Mater.* **2021**, *4*, 201.
[95] J.-Y. Lee, H.-S. Kim, J.-S. Lee, C.-J. Park, W.-H. Ryu, *ACS Sustainable Chem. Eng.* **2019**, *7*, 16151.
[96] J. Sun, Y. Huang, W. Wang, Z. Yu, A. Wang, K. Yuan, *Electrochim. Acta* **2008**, *53*, 7084.
[97] D. Choi, K. L. Choy, *Mater. Des.* **2020**, *191*, 108669.
[98] K. W. D. K. Chandrasiri, M. D. C. D. Jayawardana, M. Y. Abeywardana, J. Kim, B. L. Lucht, *J. Electrochem. Soc.* **2019**, *166*, A4115.
[99] Y. Tang, J. Deng, W. Li, O. I. Malyi, Y. Zhang, X. Zhou, S. Pan, J. Wei, Y. Cai, Z. Chen, X. Chen, *Adv. Mater.* **2017**, *29*, 1701828.
[100] H. Wang, P. Zheng, H. Yi, Y. Wang, Z. Yang, Z. Lei, Y. Chen, Y. Deng, C. Wang, Y. Yang, *Macromolecules* **2020**, *53*, 8539.
[101] H. Wang, Y. Yang, P. Zheng, Y. Wang, S.-W. Ng, Y. Chen, Y. Deng, Z. Zheng, C. Wang, *Chem. Eng. J.* **2020**, *395*, 124981.

[102] H. Wang, Y. Wang, P. Zheng, Y. Yang, Y. Chen, Y. Cao, Y. Deng, C. Wang, *ACS Sustainable Chem. Eng.* **2020**, *8*, 12799.
[103] X. Fu, L. Scudiero, W.-H. Zhong, *J. Mater. Chem. A* **2019**, *7*, 1835.
[104] J. Qiu, S. Wu, Y. Yang, H. Xiao, X. Wei, B. Zhang, K. N. Hui, Z. Lin, *ACS Appl. Mater. Interfaces* **2021**, *13*, 55092.
[105] H. Yuan, J.-Q. Huang, H.-J. Peng, M.-M. Titirici, R. Xiang, R. Chen, Q. Liu, Q. Zhang, *Adv. Energy Mater.* **2018**, *8*, 1802107.
[106] S.-L. Chou, Y. Pan, J.-Z. Wang, H.-K. Liu, S.-X. Dou, *Phys. Chem. Chem. Phys.* **2014**, *16*, 20347.
[107] J. Song, M. Zhou, R. Yi, T. Xu, M. L. Gordin, D. Tang, Z. Yu, M. Regula, D. Wang, *Adv. Funct. Mater.* **2014**, *24*, 5904.
[108] L. Kong, Y. Li, W. Feng, *Electrochem. Energy Rev.* **2021**, *4*, 633.
[109] J. Duan, X. Tang, H. Dai, Y. Yang, W. Wu, X. Wei, Y. Huang, *Electrochem. Energy Rev.* **2020**, *3*, 1.

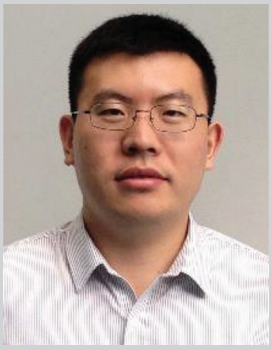

Bing Sun received his Ph.D. in 2012 at University of Technology Sydney (UTS), Australia. Currently, Dr. Sun is a research associate in the Centre for Clean Energy Technology at UTS. His research interests focus on the development of next-generation battery materials and technology for lithium-based batteries and sodium-based batteries. He is the recipient of Australian Research Council (ARC) Discovery Early Career Researcher Award (DECRA).

Guoxiu Wang is the Director of the Centre for Clean Energy Technology and a Distinguished Professor at University of Technology Sydney (UTS), Australia. Prof. Wang is an expert in materials chemistry, electrochemistry, energy storage and conversion, and battery technologies. His research interests include rechargeable batteries, supercapacitors, 2D materials, and electrocatalysis for hydrogen production. Prof. Wang has published more than 650 journal papers. His publications have attracted over 60 000 citations with an h-index of 134. He has been recognized as a highly cited researcher in Materials Science by Clarivate Analytics in 2018, 2019, 2020, and 2021.